Classical Lattice-Boltzmann Methods for fluid dynamics

Pierre Sagaut
M2P2 Laboratory
Aix-Marseille University
38 rue Joliot-Curie
Marseille cedex 13, 13013
France

pierre.sagaut@univ-amu.fr

Contents

1.0 INTRODUCTION TO LATTICE-BOLTZMANN METHOD

This lecture is devoted to the presentation of Lattice Boltzmann Methods (LBM) for Computational Fluid Dynamics [1–4], with emphasis on its use for engineering purposes. The main features and properties of LBM will be discussed in order to point the generic structure of all LBM, making it possible to analyze the issues that may arise when addressing their extension for Quantum CFD.

Here, it is worth noting that several classes of extensions may be identified:

- **Type I:** Extension of classical Lattice methods for the simulation of quantum systems (e.g. solving the Schrödinger equation) using classical algorithms/computers.
- **Type II:** Extension of classical Lattice methods for the simulation of quantum systems using quantum algorithms/computers.
- **Type III:** Extension of classical Lattice methods for the simulation of classical systems using quantum algorithms/computers.

Despite Type II methods may lead to some relevant results in the field of theoretical physics (e.g. simulation of macroscopic hydrodynamic behavior of superfluids, including superfluid turbulence), at present time the main challenge for the design of efficient Quantum CFD LBM-like approaches for applied engineering is to design methods belonging to Type III. One of the main reason for that is that engineering applications require a fine tuning the dissipative and dispersive features of the numerical methods along with the addition of a huge number of physical submodels to the basic governing equations: boundary conditions, turbulence models, turbulent wall models ... All of them having been obtained thanks to a tremendous amount of work during the last 50 years. Therefore, a ”short-to-mid-term” view should be based on the fact that Quantum CFD should inherit these results of classical CFD as much as possible, quantum computing being seen as a way to gain an additional speedup versus classical computers.

The possibility to predict macroscopic states of full scale engineering systems via the simulation of quantum systems on quantum computers should be kept in mind as a long-term perspective, since it will requires to design

large-scale quantum computers along with fully renewed submodels that will necessitates decades of effort to be calibrated to satisfy engineering constraints related to accuracy and robustness.

An hybrid path could be to use classical computers with quantum-based accelerators, in a way similar to the CPU-GPU hybrid architectures.

1.1 The 3 historical paths to LBM

Lattice Boltzmann Methods inherit from a 50 years-long tradition in mathematics, physics and scientific computing. Looking at the recent state-of-the-art, one can distinguish at least 3 main steps, corresponding to changes in the fundamental paradigm that was used to develop this numerical method.

1.1.1 The Lattice Gas Automata era

The first step consists of the development of cellular automata, which yielded the Lattice Gas Automata (LGA) approach. Cellular automata, popularized by the famous article by Gradner in 1970 about John Conway's "Game of Life" [5], have first been as implementations of Türing machine (an automaton acting as a universal computing machine), and were used to address many theoretical topics such as algorithmics, theoretical computer theory, thermodynamics of computation, possibility for self-duplicating machines and many more, e.g. [6–9]

To illustrate this point, we remind below the rules of Conway's Game of Life

- **Births**: Each dead cell adjacent to exactly three live neighbors will become live in the next generation.
- **Death by isolation**: Each live cell with one or fewer live neighbors will die in the next generation.
- **Death by overcrowding**: Each live cell with four or more live neighbors will die in the next generation.
- **Survival**: Each live cell with either two or three live neighbors will remain alive for the next generation.

It is striking that with such a simple automata all logical functions/gates (AND, NOT ...) can be implemented (see Fig.1), leading to the possibility to "build" a universal 2D computer based on this cellular automata [10].

A Lattice Gas Automaton is a cellular automation that is interpreted as a microscopic model for a gas based on Boolean unknowns (the interested reader is referred to [11**?** –13] for a deeper analysis of LGA). At each grid node one defines a lattice made of a finite number neighbouring points to which it is connected. A particule can come from/go to lattices points, and at each time step collisions can take place. After collision, colliding particles are assumed to travel with new velocities toward points of the lattice. Here, one can see that such an automaton has two degrees of freedom, namely the lattice topology and the collision rules. In 2D, on a uniform Cartesian grid, restricting the lattice stencil to the first neighbours, one can define a 5-point lattice and a 9-point lattice. On an hexagonal grid, one can define a 7-point lattice. Lattices with more points can be defined by considering neighbours of neighbouring points. The collision rules (the ancestor of the collision model in modern LBM) were historically derived to mimic elastic collisions of hard spheres. Important steps in the development of LGA for hydrodynamics were the Hardy-Pomeau-Pazzis (HPP) model [14] (based on uniform Cartesian grids, i.e. 5-point lattice with 4 velocities) later improved by the Frisch-Hasslacher-Pomeau (FHP) model [15] (based on triangular cells, i.e. 7-point lattice with 6 velocities), see Fig. 2.

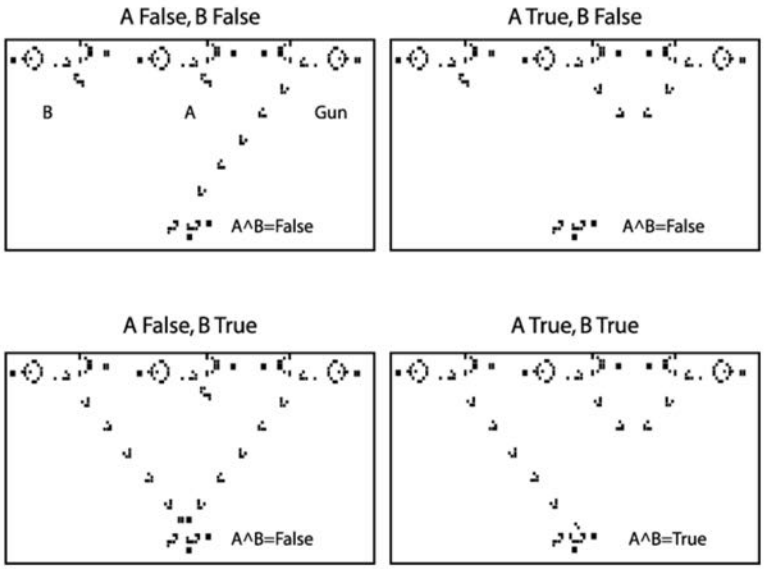

Figure 1: Examples of the AND-gate implemented via Conway's Life automaton for various inputs. From [10].

We now illustrate these methods considering the HPP LGA. Introducing a set of 4 admissible velocities and the Boolean variables $\sigma(i,j;n)$ such that

$$\sigma(i,j,k;n) = \begin{cases} 1 & \text{if the site (i,j) is occupied by a particule with velocity number n at iteration k} \\ 0 & \text{otherwise} \end{cases} \tag{1}$$

the time evolution of $\sigma(i,j,k;n)$ is governed by the following rules:

$$\sigma(i,j,k+1;1) = \sigma(i-1,j,k;1) - \Psi(i,j,k) \tag{2a}$$
$$\sigma(i,j,k+1;2) = \sigma(i,j-1,k;2) + \Psi(i,j,k) \tag{2b}$$
$$\sigma(i,j,k+1;3) = \sigma(i+1,j,k;3) - \Psi(i,j,k) \tag{2c}$$
$$\sigma(i,j,k+1;4) = \sigma(i,j+1,k;4) + \Psi(i,j,k) \tag{2d}$$

where the collision operator is defined as

$$\begin{aligned} \Psi(i,j,k) \quad = \quad & \sigma(i-1,j,k;1)\sigma(i+1,j,k;3)\bar{\sigma}(i,j-1,k;2)\bar{\sigma}(i,j+1,k;4) \\ & -\bar{\sigma}(i-1,j,k;1)\bar{\sigma}(i+1,j,k;3)\sigma(i,j-1,k;2)\sigma(i,j+1,k;4) \end{aligned} \tag{3}$$

where $\bar{\sigma}(i,j,k;n) = 1 - \sigma(i,j,k;n)$. The sum of the collision operator over the 4 velocities at a given node (i,j) is always null. It allows for the conservation of both the number of particules (i.e. mass conservation) and the total momentum.

Lattice Gas Automata have mostly been used as "experimental devices" in theoretical physics, since they exhibit some statistical features of real fluid. A Boltzmann-like kinetic theory can be build for them, along with

a statistical thermodynamic theory [16]. As an example, time evolution of LGA satisfies an H-theorem. It can be shown [17] that on a 2D hexagonal lattice, if all particules have the same speed and obey Fermi statistics, then the allowed collisions lead to a Fermi-Dirac single-particule equilibrium with distribution function

$$f_n^{eq} = \frac{1}{1 + e^{\alpha + \boldsymbol{\beta} \cdot \mathbf{e}_n}} \tag{4}$$

where $\mathbf{e}_n$ is the particule velocity in the n-th direction and α and $\boldsymbol{\beta}$ are determined by the conservation law. In the limit of small velocity, this equilibrium can be expanded in dimension D as follows:

$$f_n^{eq} = \frac{\rho}{b} + \frac{\rho D}{c^2 b} \mathbf{e}_n \cdot \mathbf{u} + \frac{\rho D(D+2)}{2c^4 b} G(\rho) Q_{ijn} u_i u_j + O(u^3), \quad Q_{ijn} = e_{ni} e_{nj} - 1/D \delta_{ij} \tag{5}$$

where ρ and $\mathbf{u}$ denote the averaged density particule per site and the averaged particule velocity per site, respectively. The function $G(\rho)$ depends on both the dimension and the lattice topology. c is the particle speed which is equal to one lattice unit per lattice time for a hexagonal lattice, and b is the number of allowed velocities for particules. Associated macroscopic equations can also be derived via a multi-scale analysis, which resemble the Navier–Stokes equations. For the above equilibrium, one obtains the following macroscopic momentum equation:

$$\frac{\partial}{\partial t}(\rho u_i) + \frac{\partial}{\partial x_j}(\rho G(\rho) u_i u_j) = -\frac{\partial}{\partial x_j} p + \frac{\partial}{\partial x_i}\left(\nu \frac{\partial}{\partial x_j}(\rho u_i)\right) + \frac{\partial}{\partial x_j}\left(\zeta \frac{\partial}{\partial x_i}(\rho u_i)\right) \tag{6}$$

where ν and ζ are the kinematic viscosity and the bulk viscosity, respectively. The associated equation of state is

$$p = \frac{c^2 \rho}{D}\left(1 - G(\rho)\frac{u^2}{c^2}\right) \tag{7}$$

One can see that these macroscopic equations are unphysical with respect to classical laws because 1) Galilean invariance is broken by the appearance of $G(\rho)$ and 2) the pressure depends on the velocity $\mathbf{u}$.

Despite the fact that they can be very easily implemented and that they are numerically unconditionally stable (thanks to their Boolean nature), LGA never became a quantitative predictive tool in Computational Fluid Dynamics. The main problems are that

- they lead to noisy results (due to their Boolean character, statistical moments of the solution converge very slowly)
- they do not converge toward Galilean-invariant macroscopic equations
- the equation of state is unphysical because of $G(\rho)$
- a spurious conserved quantity is present because of the simple symmetry of the lattice of LGA

In order to alleviate these shortcomings, Lattice Gas Automata with enriched, more physical collision rules have been proposed. Among the first proposals, one can mention sequels of the FHP model, in which the collision rules are complexified (see [19] for a review of these advanced variants). The concept of Integer LGA (ILGA) was later introduced in 1997 (so after the rise of classical LBM) by Boghosian et al. [20] to allow for an arbitrary number of particules to travel in the same direction. Increasing the number of sampled particules, better collision statistics may be obtained. Doing that, Galilean invariance is restored and an expression for

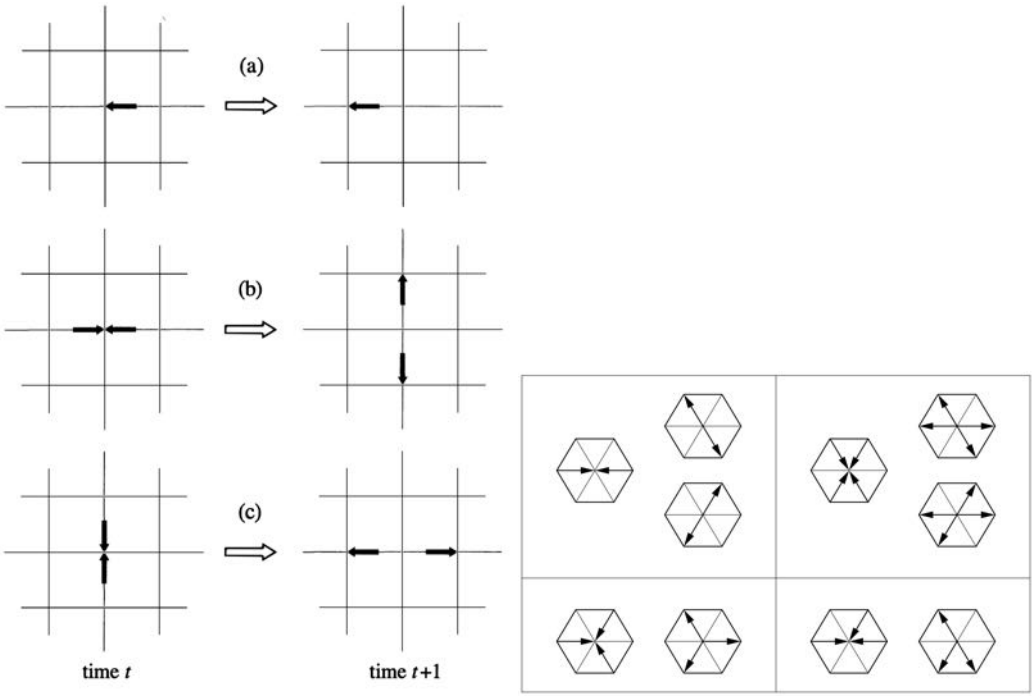

Figure 2: Lattice Gas Automata collision rules: HPP (left, from [12]) and FHP (right, from [18])

the fluid viscosity is explicitly derived, along with a decrease of the statistical noise. Integer LGA were further improved in 2018 by Blommel and Wagner [21] who proposed the Monte Carlo LGA, whose key idea is to use a Monte Carlo collision operator (therefore further increasing the number of samples used to compute the collision) that explicitly conserves mass and momentum, and which recovers the correct equilibrium function, reinforcing the link with Lattice Boltzmann Methods. During the same period, Parsa and Wagner developed the Molecular Dynamics LGA (MDLGA) in which the collision operator is computed by coarse-graining a Molecular Dynamics simulation [18, 22–28]. Here, the sampling is made more physical since particules in the MD simulation are allowed to move freely in space and are not restricted to follow a set of discrete directions as in other LGA methods (see Fig. 3). The coarse-graining step is done by averaging the Molecular Dynamics results in each cell of the lattice. On can show that resulting collision operator (and equilibrium state) is the one that LBM collision operator asymptotically approximates. In this sense, one can say that MDLGA and LBM are asymptotically statistically similar (at least at equilibrium), if not equivalent (but there are many collision models in the LBM approach, see below).

It is also interesting to note that some trials have been made to use LGA to describe other physical systems, such as magnetohydrodynamics, plasma physics and wave propagation (see [29] for a survey).

1.1.2 The birth of LBM as a discretized fluid model

The Lattice Boltzmann Methods were born in the late 1980s and the early 1990s thanks to seminal papers by McNamara and Zanetti [30], Qian, D'Humières and Lallemand [31] and Higuera et al. [32, 33]. The later is often considered as the birth record of modern LBM, since the McNamara-Zanetti and Higuera papers are very brief and don't provide enough details about collision terms and practical implementation.

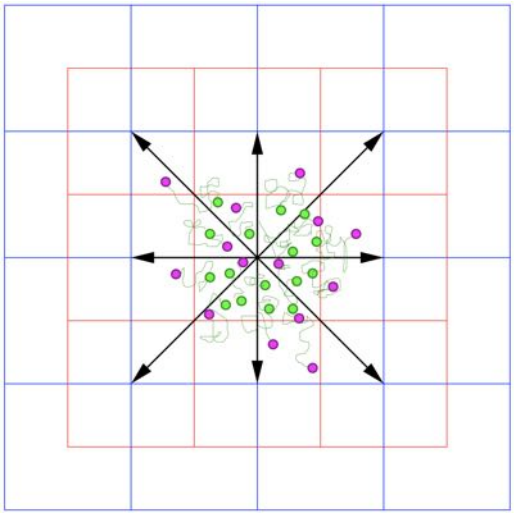

Figure 3: Molecular Dynamics Lattice Gas collision. Coarse grid cells are in blue, the dual grid is in orange. Particules of the Molecular Dynamics simulation are shown. From [22].

In order to cure the flaws of LGA, it is proposed to use real variables instead of Boolean ones (therefore removing noise) and by expressing the collision operator as a relaxation process toward an equilibrium state, the expression of the later originating in a truncated polynomial expansion of the classical continuous Maxwellian. This change amounts to switch from a microscopic view in which individual collisions are simulated (and the equilibrium state is a by-product) to a mesoscopic approach based on density probability functions in which the equilibrium state is arbitrarily chosen and enforced. Using such a collision model, Galilean invariance of macroscopic equations is enforced and the usual Euler and Navier–Stokes are recovered. The final form of modern LBM appears in [31] for the first time to the knowledge of the author, including the nomenclature for the lattices was introduced in this article: a lattice with n points in m dimension is denoted $DmQn$.

Important facts are that LBM is not an LGA and that it is a quantitative predictive tool that provide reliable results for engineering purposes.

These seminal works were carried out within the discrete velocity framework inherited from the LGA structure. A last very important step was to derive the LBM directly from the continuous Boltzmann equation, i.e. to show that LBM can be seen as a numerical method to solve the continuous Boltzmann equation. This step was done in the mid 1990s in two seminal papers [34, 35] (see also [4, 36] for reviews). This way, the link with classical hydrodynamic theory and kinetic theory is established, and LBM can be analyzed a a classical numerical method using usual tools. To this end, LBM schemes are obtained considering a triple discretization procedure in the velocity space (phase space), in space and time. The discretization in velocity space yields the Discrete Velocity Boltzmann Equation (DVBE), whose further discretisation is space and time leads to LBM. Let us note that the convergence of DVBE toward Boltzmann equation and Navier–Stokes equations is an active research topic . The asymptotic consistency of LBM with both nearly incompressible Navier–Stokes equations and rarefied gas dynamics is also a theoretical issue, referred to as the asymptotic preserving properties [37]. Let us just mention that all LBM schemes are not asymptotic preserving.

Once a computational grid has been defined, DVBE can be discretized and solved using any usual method: Finite Difference, Finite Volume, Finite Element, Discontinuous Galerkin, Pseuso-spectral methods, Galerkin Least-Square ... As a matter of fact, all these methods have been applied to DVBE since the 1990s. Using these

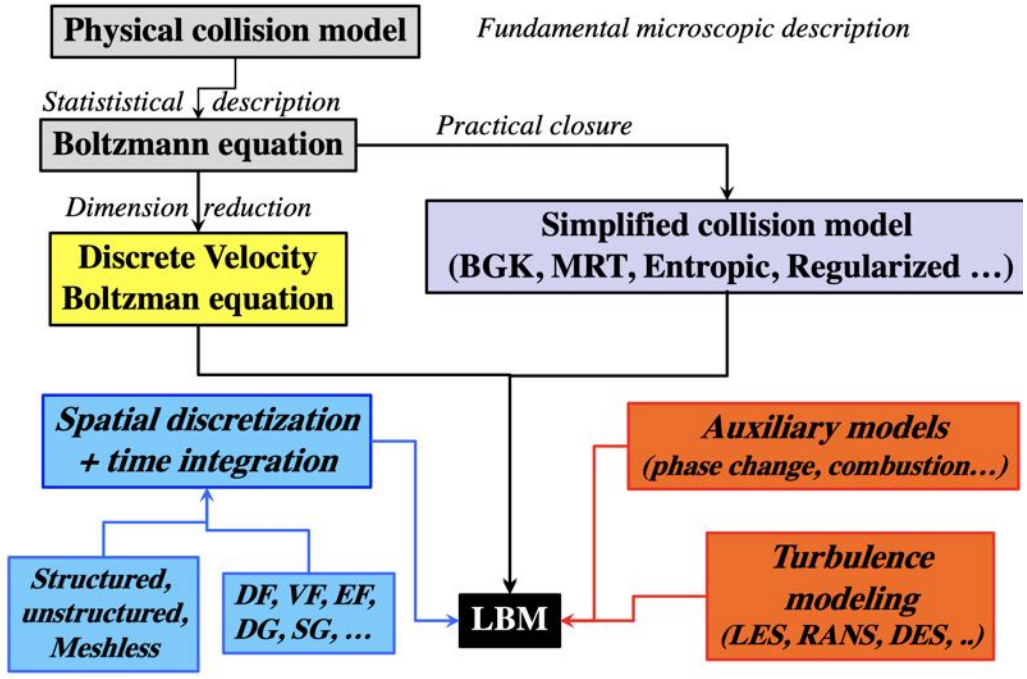

Figure 4: General sketch of the different choices leading to an LBM method starting from the continuous Boltzmann equation.

approaches, the constraint to use regular lattices, i.e. uniform computational grids inherited from LGA, was removed, and all grid topologies have been used: structured, unstructured, body-fitted, non-body-fitted ... and also gridless methods.

What is referred to as Lattice Boltzmann Methods is observed to stem from a particular choice of discretization, which preserves the collide-and-stream structure, the streaming step being done via a simple shift in memory (see Section 2.0). Other methods are not LBM *stricto sensu*, and there exist a broad panel of methods that share some features of LBM but are not LBM and whose names are misleading, e.g. Finite Volume LBM whose correct name should be Finite Volume DVBE (the same for Finite Element LBM ...) A general sketch of the choice graph that leads to LBM is displayed in Fig. 4.

LBM is now widely spread among CFD teams and is a mature CFD approach. It has been extended to a large class of flows, among which compressible flows, multiphase flows, combustion ... Commercial CFD softwares have been developed (e.g. Powerflow, ProLB, Xflow) that are observed to challenge traditional CFD solvers, thanks to some beneficial features: very small spurious numerical dissipation and dispersion, high scalability on massively parallel computer, compactness of lattices, automatic generation of computational grid .... Some illustrations are given in Section 1.2. Let us mention that the search for improved LBM schemes with increased efficiency is a very active field of research.

1.1.3 The renewal of LBM as a general numerical method

The last mutation of LBM was to decouple it from fluid mechanics and to show that it is a general numerical approaches that can be used to solved a large family of PDEs that are not tied to fluid mechanics and that even do not belong to mathematical physics. As a matter of fact, searching for improved LBM schemes, researchers

have proposed collision models that cannot be obtained from the continuous Maxwellian for a long time. But, in most of the cases, these improved collision schemes were presented as empirical modifications of pre-existing methods or as plugs of classical numerical tools (e.g. slope limiters in CFD) without a general theoretical framework. In the same way, LBM-like methods for solving non-hydrodynamic equations (solid mechanics, Maxwell equations ... epidemiology) have been proposed in isolated ways, as illustrated by Section 3.0.

Decoupling LBM from fluid mechanics and making it a general numerical approach is the most recent renewal of this field of research. Here, LBM is mainly seen as a smart change of variables which

1. change/increase the number of unknowns of the problem
2. convert the original set of macroscopic PDEs into a set of coupled advection-relaxation equations, with linear advection and nonlinear local relaxation

The key step is to keep in mind that convergence toward a given macroscopic equation is governed by a few consistency constraints, and that numerical efficiency (accuracy, robustness, computational cost) are additional constraints. To tune adequately LBM, one has to derive generic equations for the associated macroscopic model and to use classical theoretical tools of numerical analysis (Equivalent Differential Equation obtained via Taylor expansion [38], Von Neumann-like Linearized Spectral Analysis [38, 39], structure-preserving features [40]). This approach is the one selected for the present survey.

Re-embedding LBM within the general CFD framework offers new perspectives in terms of theoretical analysis but also in terms of ways of improvement. Hybridization with classical numerical techniques [41–46] or finding numerical schemes for macroscopic equations that are equivalent from the discrete point of view to a given LBM scheme (and which exhibit the same features in terms of accuracy, robustness, efficiency) are very active fields of research to derive improved LBM-like numerical schemes, e.g. [47–49].

1.2 LBM for applied CFD: a (brief) survey

As mentioned above, Lattice Boltzmann Methods are predictive methods that can be used for engineering purposes. Main applications are driven by the availability of both adequate LBM schemes and user-friendly softwares. The first commercial CFD software based on LBM to reach the market about 20 years ago was PowerFlow (by Exa Corporation, now Dassault Systems) with application to automotive industry (more precisely for aerodynamics, heat transfer and aeroacoustics of vehicules), then followed about 10 years ago by ProLB and Xflow, see Fig. 5. As a consequence, very efficient methods for low-Mach weakly compressible flows have been developed to get a reliable engineering tools. An important point is that coupling with a large number of physical submodels (e.g. turbulence models) have been developed, along a many numerical elements such as boundary conditions [50–52], grid refinement [53–56], immersed boundary conditions [57], multiple reference frame approach for rotating bodies [58, 59] and stabilized LBM schemes for highly convective flows (basic LBM schemes are not stable in such flows, all realistic applications rely on advanced LBM models, see Section 4.3).

A by-product of these developments is the capability of LBM to be an efficient tools for other family of applications that exhibit the same physics as automotive industry, e.g. urban physics, wind engineering, micrometeorology and air quality (see Figs. 7 and 6) [60–64]. Some dedicated LBM software for urban physics have been developed, e.g. Simscale.

The second market addressed by developers of commercial LBM softwares was aerospace engineering (see Fig. 8), leading to the development of LBM schemes for compressible flows, including supersonic flows with shocks, e.g. [42–46, 66–71]. All-Mach number LBM schemes do not exist [72], and the state-of-the-art shows

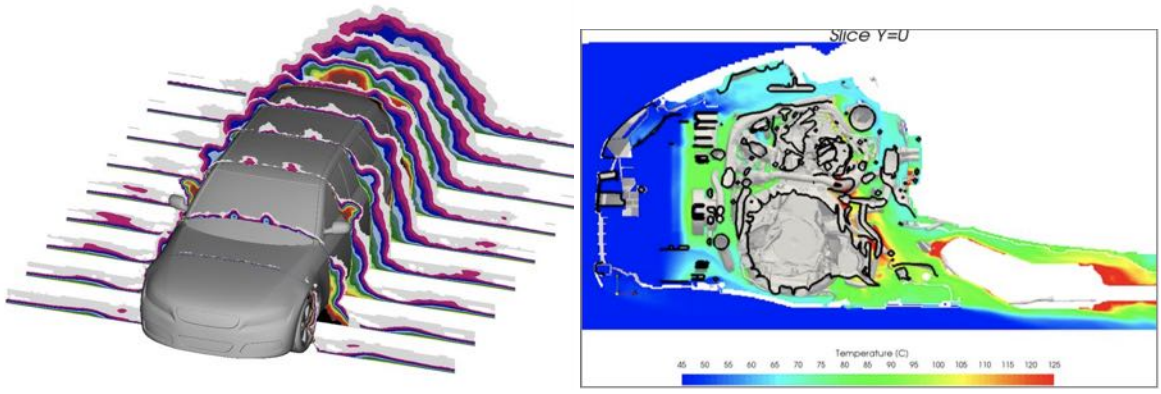

Figure 5: Illustration of LBM simulations in automotive engineering. Left: simulation of the flow around a car for aerodynamics; Right: flow in underhood for heat transfer and engine cooling. Courtesy of Renault and CS. All simulations have been carried out with the ProLB software.

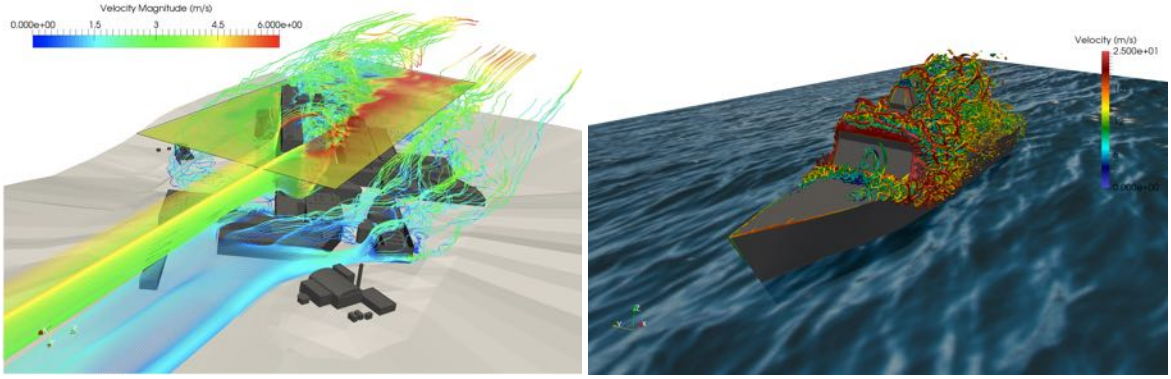

Figure 6: Illustration of LBM simulations in wind engineering. Left: flow in an urban area; Right: flow around a Fregate ship. Courtesy of M2P2 Laboratory. All simulations have been carried out with the ProLB software.

that different collision models should be used for subsonic flows and compressible flows. At present time, LBM for hypersonic flows is still at an embryonic stage of development, since the demand is weak. Extension to combustion (which is a crucial topic for the design of aircraft/helicopter/missile engines) is presently underway [73–80], the ProLB software being the first one to offer combustion capabilities (see Fig. 9). An important point is that the development of efficient LBM schemes that account for the energy equation is a non-trivial task, since a direct extension of low-Mach athermal LBM schemes leads to the use of a huge number of degrees of freedom (more than 130 unknowns per cell in practice in 3D simulations). Decreasing the number of unknowns requires the development of segregated methods, in which the energy equation is treated in a separate way. The difficulty dealing with the definition of fully conservative methods based on total energy, which is mandatory for shock capturing, was solved very recently in [43, 70, 81].

The last main field of application is oil and gas, which led to the development of efficient LBM schemes for multiphase multispecies flows, including physical mechanisms such as evaporation, melting and solidification (see [82] for a review).

One should also mention applications of LBM to bio-mechanics [83–87], including non-Newtonian fluids

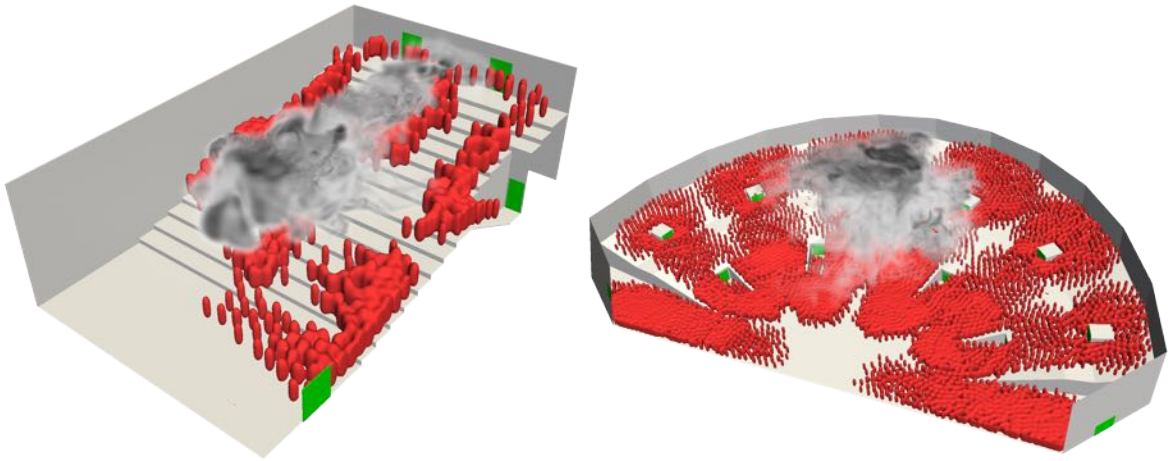

Figure 7: Illustration of LBM simulations air quality engineering. Evacuation of a cinema room (left) and a concert hall (right) accounting for person's displacement. From [65]. All simulations have been carried out with the ProLB software.

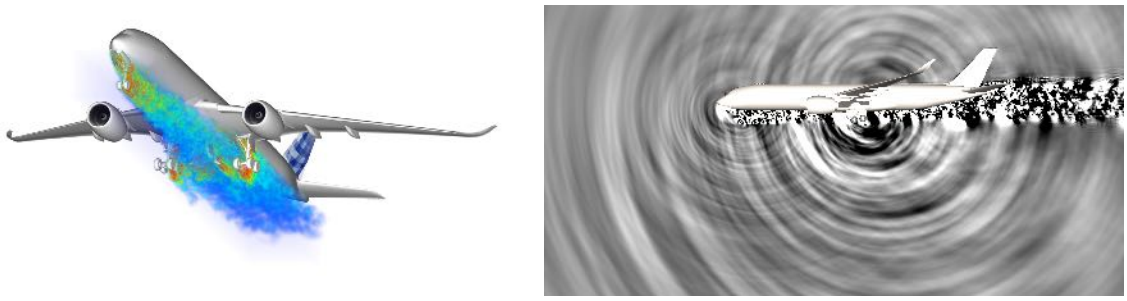

Figure 8: Illustration of LBM simulations in aerospace engineering. Left: take-off of A350 aircraft; Right: noise generated by landing gears on a full aircraft configuration during landing. Courtesy of Airbus. All simulations have been carried out with the ProLB software.

[88] and fluid-structure interaction [89–95].

1.3 LBM as a general numerical method: beyond CFD

The fact that LBM can be used to solve PDEs that do not describe classical fluid dynamics (i.e. systems that totally escape the physics underlying the development of statistical physics and kinetic theory) has been recognized since a long time, despite a general theory for "LBM numerics" is still missing.

Among the most striking achievements, one can mention:

- LBM for solid mechanics, with emphasis on wave propagation in elastic solids ans seismic simulations, e.g. [96–98].
- LBM for Maxwell equations for electrodynamics [99, 100], with emphasis on electromagnetic wave propagation, with extension to magnetohydrodynamics (MHD) [101–108]

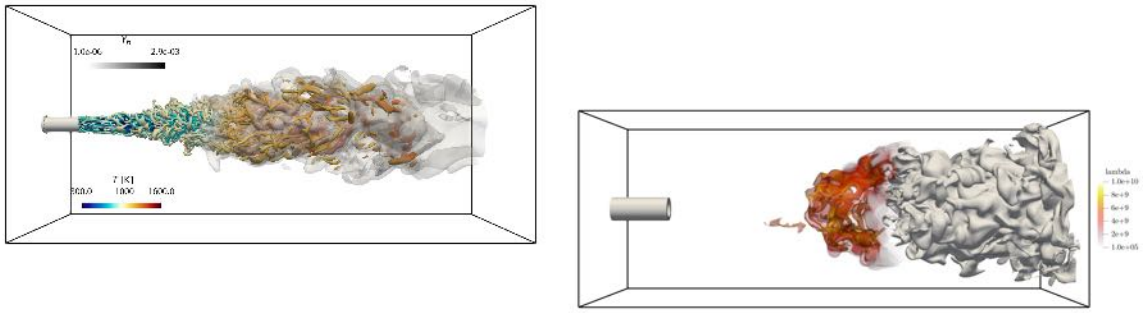

Figure 9: Illustration of LBM simulations for combustion. Left: reactive turbulent jet; Right: turbulent jet with auto-ignition. Courtesy of M2P2 Laboratory. All simulations have been carried out with the ProLB software.

- LBM for heat transfer, including conduction and radiative transfer equations, e.g. [109–112]
- LBM for relativistic fluids with application to astrophysics, e.g. [113–115]
- LBM for shallow water equations, with application to environmental flows, e.g. river simulation including topography effect, erosion, sediment transport and tsunami simulation, e.g. [116–121]
- LBM for miscellaneous topics, e.g. epidemics [122] and crowd dynamics [65, 123, 124]
- LBM for Dirac and Schrödinger equations, superfluid hydrodynamics and quantum turbulence (See Section 6.0)

2.0 IMPLEMENTING LATTICE-BOLTZMANN METHOD

This section discuss the derivation and implementation of a generic Lattice Boltzmann Method to solve a set of PDEs. It follows the recent works by G. Farag and G. Wissocq and colleagues at M2P2 laboratory, see [42, 43, 125–130].

2.1 A generic Discrete Velocity Boltzmann Equation (DVBE)

Lattice Boltzmann Methods rely on the Discrete Velocity Boltzmann equation, which is very often interpreted as a discretization of the continuous Boltzmann equation in the velocity space [34–36, 131]. This interpretation is inherited from the history of LBM, as mentioned above, and also from the works dealing with discretization of kinetic equations for fluid mechanics, e.g. [132–138]. This interpretation is no longer true when LBM is used to discretize macroscopic governing equations that have no link with statistical gas kinetic theory (e.g. solid mechanics, Schrödinger equation ...) It is important to keep in mind that the DVBE is still continuous in time and space and therefore require to be further discretized to allow for numerical simulation. A generic DVBE based on a set of N discrete velocities $\mathbf{c}_i$ can be written as follows

$$\frac{\partial f_i}{\partial t} + c_{i\alpha}\frac{\partial f_i}{\partial x_\alpha} = \Omega_i, \quad i = 0, N-1, \quad \alpha = 1, 3 \tag{8}$$

where $f_i(t,\mathbf{x}) = f(t,\mathbf{x},\mathbf{c}_i)$ and Ω_i denote the distribution function associated to the discrete velocity $\mathbf{c}_i$ and its collision term, respectively. It is worth noting that since discrete velocities are constant, uniform, f_i-independent variables, the advection operator in (8) is linear. The collision term is a priori non-linear in the general case. It is local in both space and time in newtonian fluid mechanics.

The link with a targeted system of macroscopic equations is usually obtained introducing Grad's raw moments of the distribution functions and the collision terms in the velocity space:

$$\mathbf{\Pi}^{f,(n)}_{\alpha_1\cdots\alpha_n} = \sum_i c_{i\alpha_1}\cdots c_{i\alpha_n} f_i, \quad \mathbf{\Pi}^{\Omega,(n)}_{\alpha_1\cdots\alpha_n} = \sum_i c_{i\alpha_1}\cdots c_{i\alpha_n}\Omega_i \tag{9}$$

This corresponds to a linear transformation (or change of variables)

$$\left(\mathbf{\Pi}^{f,(j)}\right)_{j=0,P-1} = M(f_j)_{j=0,N-1} \tag{10}$$

where the matrix M, whose elements are polynomial functions of the components of the discrete velocity vectors $\mathbf{c}_i$, is invertible if $M = N$, i.e. if the number of moments is equal to the number of distribution functions (which is equal to the number of discrete velocities).

Taking the N-th first moments of Eq. (8), one obtains evolution equations for the $\mathbf{\Pi}^{f,(n)}_{\alpha_1\cdots\alpha_n}$:

$$\frac{\partial \mathbf{\Pi}^{f,(n)}_{\alpha_1\cdots\alpha_n}}{\partial t} + \frac{\partial \mathbf{\Pi}^{f,(n+1)}_{\alpha_1\cdots\alpha_{n+1}}}{\partial x_{\alpha_{n+1}}} = \mathbf{\Pi}^{\Omega,(n)}_{\alpha_1\cdots\alpha_n}, \quad n = 0, N-1 \tag{11}$$

This set of equations is strictly equivalent to system (8). It is observed that it is not closed, since the unknown moments $\mathbf{\Pi}^{f,(N)}_{\alpha_1\cdots\alpha_N}$ appears in the equation for the last known moment, $\mathbf{\Pi}^{f,(N-1)}_{\alpha_1\cdots\alpha_{N-1}}$. Therefore, a closure will be needed to obtain a computable solution.

Its is worth noting that, at this point, both systems (8) and (11) are fully general and are not tied to fluid mechanics. Choosing the set of targeted macroscopic equations to be solved via LBM amounts 1) to bridge between moments of f and the macroscopic variables and 2) giving an expression for the collision operators Ω_i. Before deriving the macroscopic equations, it is useful to split f_i as

$$f_i = f_i^{eq} + f_i^{neq}, \tag{12}$$

where f_i^{eq} is such that $\Omega_i(f_i^{eq}) = 0$. An important point is that f_i^{eq} is a function of macroscopic variables only. Moments of f_i can be split in the same way, yielding

$$\mathbf{\Pi}^{f,(n)}_{\alpha_1\cdots\alpha_n} = \mathbf{\Pi}^{f^{eq},(n)}_{\alpha_1\cdots\alpha_n} + \mathbf{\Pi}^{f^{neq},(n)}_{\alpha_1\cdots\alpha_n}. \tag{13}$$

In classical kinetic gas theory, f_i^{eq} is related to the Maxwell-Boltzmann equilibrium, for which the entropy is stationary and the collision term vanishes. Inserting this decomposition into Eqs. (8) and (11), one obtains in a straighforward way:

$$\frac{\partial f_i^{eq}}{\partial t} + c_{i\alpha}\frac{\partial f_i^{eq}}{\partial x_\alpha} = 0, \tag{14a}$$

$$\frac{\partial f_i^{neq}}{\partial t} + c_{i\alpha}\frac{\partial f_i^{neq}}{\partial x_\alpha} = \Omega_i, \tag{14b}$$

and

$$\frac{\partial \mathbf{\Pi}^{f^{eq},(n)}_{\alpha_1\cdots\alpha_n}}{\partial t} + \frac{\partial \mathbf{\Pi}^{f^{eq},(n+1)}_{\alpha_1\cdots\alpha_{n+1}}}{\partial x_{\alpha_{n+1}}} = 0, \tag{15a}$$

$$\frac{\partial \mathbf{\Pi}^{f^{neq},(n)}_{\alpha_1\cdots\alpha_n}}{\partial t} + \frac{\partial \mathbf{\Pi}^{f^{neq},(n+1)}_{\alpha_1\cdots\alpha_{n+1}}}{\partial x_{\alpha_{n+1}}} = \mathbf{\Pi}^{\Omega,(n)}_{\alpha_1\cdots\alpha_n}. \tag{15b}$$

Let us illustrate that using the (very popular) case of low-Mach athermal flows. The density ρ, momentum $\rho\mathbf{u}$ and momentum flux are defined as follows

$$\rho = \mathbf{\Pi}^{f,(0)} = \sum_i f_i, \tag{16a}$$

$$\rho u_\alpha = \mathbf{\Pi}^{f,(1)}_\alpha = \sum_i c_{i\alpha} f_i, \tag{16b}$$

$$(\rho u_\alpha u_\beta + p\delta_{\alpha\beta}) = \mathbf{\Pi}^{f^{eq},(2)}_{\alpha\beta} = \sum_i c_{i\alpha} c_{i\beta} f^{eq}_i \tag{16c}$$

and it is chosen to define equilibrium and non-equilibrium components such that the low-order moments of f^{neq}_i are null (up to an arbitrarily fixed order in practice, which is case-dependent). This is illustrated by the following relations, that are enforced for low-Mach athermal flow simulations:

$$\sum_i f^{neq}_i = 0 \Longleftrightarrow \sum_i f_i = \sum_i f^{eq}_i = \mathbf{\Pi}^{f,(0)} = \mathbf{\Pi}^{f^{eq},(0)} \tag{17a}$$

$$\sum_i c_{i\alpha} f^{neq}_i = 0 \Longleftrightarrow \sum_i c_{i\alpha} f_i = \sum_i c_{i\alpha} f^{eq}_i = \mathbf{\Pi}^{f,(1)}_\alpha = \mathbf{\Pi}^{f^{eq},(1)}_\alpha,\ \alpha = 1,3 \tag{17b}$$

Now inserting these definitions into (11), one obtains after some algebra

$$\frac{\partial \rho}{\partial t} + \frac{\partial \rho u_\alpha}{\partial x_\alpha} = \mathbf{\Pi}^{\Omega,(0)} = \sum_i \Omega_i \tag{18a}$$

$$\frac{\partial \rho u_\alpha}{\partial t} + \frac{\partial \left(\rho u_\alpha u_\beta + p\delta_{\alpha\beta} + \mathbf{\Pi}^{f^{neq},(2)}_{\alpha\beta}\right)}{\partial x_\alpha} = \mathbf{\Pi}^{\Omega,(1)}_\alpha = \sum_i c_{i\alpha}\Omega_i \tag{18b}$$

In order to recover governing equations of fluid mechanics, one has two mandatory constraints on the collision term, i.e.

$$\mathbf{\Pi}^{\Omega,(0)} = \sum_i \Omega_i = 0 \,\text{(mass conservation)}, \tag{19a}$$

$$\mathbf{\Pi}^{\Omega,(1)}_\alpha = \sum_i c_{i\alpha}\Omega_i = \mathbf{0} \,\text{(momentum conservation)} \tag{19b}$$

The second-order non-equilibrium moment tensor ($\mathbf{\Pi}^{f^{neq},(2)}_{\alpha\beta}$) should vanish in the case of Euler equations for inviscid flows and be equal to the viscous stress tensor in the case of Navier–Stokes equations for viscous fluids, i.e.

$$\mathbf{\Pi}^{f^{neq},(2)}_{\alpha\beta} \simeq \nu \left(\frac{\partial u_\alpha}{\partial x_\beta} + \frac{\partial u_\beta}{\partial x_\alpha} - \frac{2}{3}\delta_{\alpha\beta}\frac{\partial u_\gamma}{\partial x_\gamma} \right) = S_{\alpha\beta} \tag{20}$$

It is worth noting that defining the momentum flux is implicitly equivalent to defining the pressure p. The expression for the pressure, i.e. the equation of state underlying the DVBE will be discussed in the next subsection. But just let us note at this point that it is enslaved to the choice of both the lattice and the collision operator.

2.2 Designing the Lattice

The lattice (i.e. the set of point that are used to update the solution for one time step at a given point) is enslaved to the choice of the set of discrete velocities $\mathbf{c}_i$. It is worth noting that the later appears to be quadrature points in the velocity space when computing the moments defined in (11). These discrete velocities are chosen to fulfil the two following constraints:

- Accuracy: they should allow for an accurate computation of low-order moments required to recover the targeted macroscopic equations (second-order moments are necessary to recover Navier-Stokes equations in a consistent way).
- Lattice preservation: discrete velocities must be chosen in such a way that, when updating the solution for one time step Δt, the advection step should exactly stream the solution from the starting point to points of its lattice. This means that no interpolation step is needed as in Lagrangian-projection methods. This is expressed by the fact that if $\mathbf{x}$ is a node of the lattice (in practice a grid point in the classical CFD parlance), then $(\mathbf{x} + \mathbf{c}_i\Delta t), i = 0, N-1$ is also a point of the lattice (i.e. a grid point).

These two constraints have a deep impact on the LBM grid topology, since the computational grid must be based on a space-filling pattern: isosceles triangle, square and hexagon in 2D, platonic solids in 3D, cubic cells being used in almost all existing implementation of LBM.

Once the lattice has been designed, one must compute the corresponding quadrature rule and quadrature weights to evaluate moments in the velocity space [139–143]. As a matter of fact, considering a dummy function $\psi(\mathbf{c})$, its integral is approximated via a discrete lattice-based quadrature rule:

$$\int \psi(\mathbf{c}) d\mathbf{c} = \sum_i \omega_i \psi(\mathbf{c}_i) + \Upsilon^\psi \tag{21}$$

where Υ^ψ is the error committed when integrating ψ, ω_i is the quadrature coefficient associated to the discrete velocity $\mathbf{c}_i$. It is worth to note that these coefficients depend on the lattice. More generally, the quadrature error committed on the p-th order moment of ψ will be denoted $\Upsilon^{\psi,(p)}$, i.e.

$$\Upsilon^{\psi,(p)}_{\alpha_0\cdots\alpha_{(p-1)}} = \int c_{\alpha_0}\cdots c_{\alpha_{(p-1)}}\psi d\mathbf{c} - \sum_{i=0,N-1} \omega_i c_{i\alpha_0}\cdots c_{i\alpha_{(p-1)}}\psi \tag{22}$$

Since in LBM the discrete velocities are enslaved to the computational grid topology (to achieve the streaming step without interpolation), the sole free adjustable parameters are the weights ω_i. Therefore, one needs

$P+1$ a lattice with discrete velocities to integrate exactly a polynomial function of order P. As a consequence, for a given lattice, their exists a (finite, usually low !) maximum moment order that can be exactly computed. Increasing the order of physical moments that must be exactly computed induces a growth of the lattice size (in number of grid points and sometimes in terms of stencil size, which may render implementation more difficult).

Another important point is that the distribution function f_i appearing above is pre-multiplied by ω_i for the relations in (16) to be interpreted as discrete versions of continuous moments in the velocity space. Therefore, variables f_i (resp. Ω_i) appearing in above sections are in fact products of a "physical" distribution function (resp. collision term) and the associated quadrature coefficient.

Discrete velocities and quadrature coefficients are chosen such that (for a lattice with N points):

$$\sum_{i=0,N-1} \omega_i = 1 \tag{23}$$

$$\sum_{i=0,N-1} \omega_i c_{i\alpha} = 0 \tag{24}$$

$$\sum_{i=0,N-1} \omega_i c_{i\alpha} c_{i\beta} = c_s^2 \delta_{\alpha\beta} \tag{25}$$

$$\sum_{i=0,N-1} \omega_i c_{i\alpha} c_{i\beta} c_{i\gamma} = 0 \tag{26}$$

$$\sum_{i=0,N-1} \omega_i c_{i\alpha} c_{i\beta} c_{i\gamma} c_{i\mu} = c_s^4 (\delta_{\alpha\beta}\delta_{\gamma\mu} + \delta_{\alpha\gamma}\delta_{\beta\mu} + \delta_{\alpha\mu}\delta_{\beta\gamma}) \tag{27}$$

$$\sum_{i=0,N-1} \omega_i c_{i\alpha} c_{i\beta} c_{i\gamma} c_{i\mu} c_{i\nu} = 0 \tag{28}$$

These relations are often referred to as the symmetries of the lattice. Here, c_s is a constant related to the lattice. For a uniform grid with mesh size Δx, one has $c_s = \Delta x/(\sqrt{3}\Delta t)$. This quantity is interpreted as the lattice speed of sound in fluid flow simulations. The pressure p appearing in the definition of the macroscopic momentum flux is given by $p = \rho c_s^2$, which is not equal to the pressure appearing in the incompressible Navier–Stokes equations. This equation of state exhibit some similarity with the definition of acoustic pressure.

The D2Q9 lattice (with 9 discrete velocities in 2D on square cells) is illustrated in Fig. 10.

2.3 Space discretization, time integration, change of variables

We now address the numerical scheme that underlies LBM. Starting from (8), one can write

$$f_i(t+\Delta t, \mathbf{x}+\mathbf{c}_i\Delta t) = f_i(t,\mathbf{x}) + \int_0^{\Delta t} \Omega_i(t+s, \mathbf{x}+\mathbf{c}_i s) ds \tag{29}$$

The right-hand side is usually computed using the trapezoidal rule, leading to the Crank–Nicolson scheme [144], yielding

$$f_i(t+\Delta t, \mathbf{x}+\mathbf{c}_i\Delta t) = f_i(t,\mathbf{x}) + \frac{\Delta t}{2}\left(\Omega_i(t,\mathbf{x}) + \Omega_i(t+\Delta t, \mathbf{x}+\mathbf{c}_i\Delta t)\right) \tag{30}$$

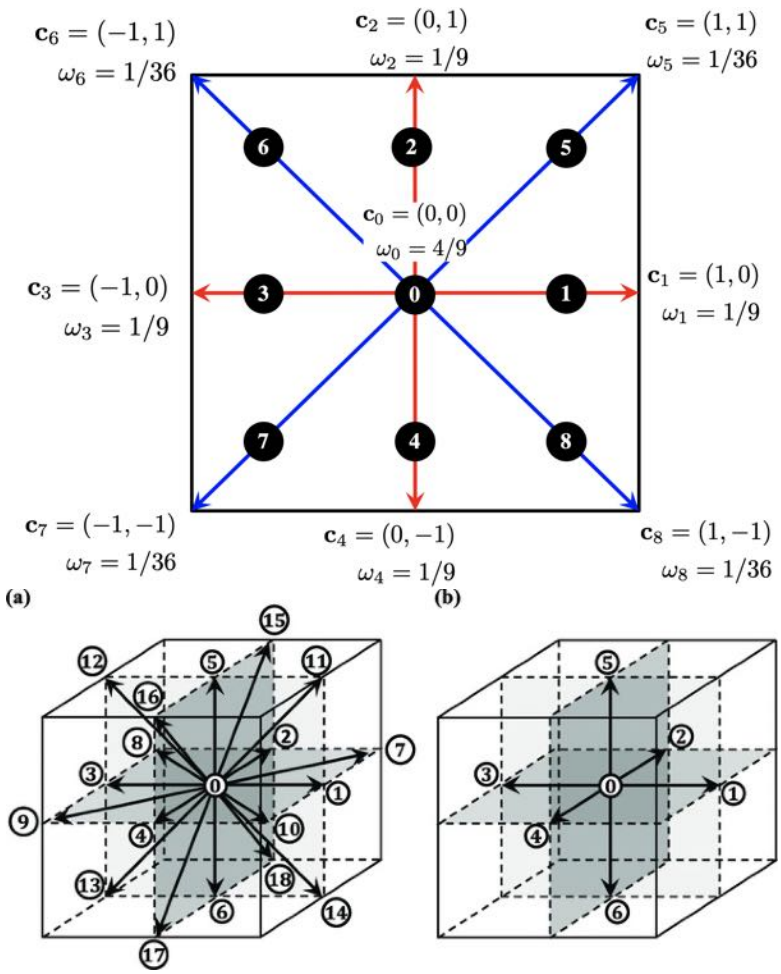

Figure 10: Sketch of the D2Q9 lattice (top) and D3Q19 and D3Q7 (bottom) .

which is a second-order accurate implicit formula, since $\Omega_i(t+\Delta t, \mathbf{x}+\mathbf{c}_i\Delta t)$ a priori depends on $f_i(t+\Delta t, \mathbf{x}+\mathbf{c}_i\Delta t)$. In order to recover an explicit method, one introduce the following change of variable:

$$g_i = f_i - \frac{\Delta t}{2}\Omega_i \tag{31}$$

Considering the case $f_i = f_i^{eq}$, one straightforwardly obtains

$$g_i^{eq} = f_i^{eq} - \frac{\Delta t}{2}\Omega_i(f_i^{eq}) = f_i^{eq} \tag{32}$$

along with

$$g_i^{neq} = g_i - g_i^{eq} = (f_i - \frac{\Delta t}{2}\Omega_i) - f_i^{eq} = f_i^{neq} - \frac{\Delta t}{2}\Omega_i \tag{33}$$

These relations shows that all moments of f_i^{eq} and g_i^{eq} are identical, while those of f_i^{neq} and g_i^{neq} are equal up to the maximum order at which the moment of the collision term vanish.

Inserting this into (30), one obtains the following explicit formula

$$g_i(t+\Delta t, \mathbf{x}) = g_i(t, \mathbf{x} - \mathbf{c}_i\Delta t) + \Delta t \Omega_i(t, \mathbf{x} - \mathbf{c}_i\Delta t) \tag{34}$$

This expression is fully general and doesn't rely on some particular expression of the collision term Ω_i. For hydrodynamic simulations, accounting for the relations (19), one can see that macroscopic variables can be easily computed:

$$\rho = \sum_i f_i = \sum_i g_i, \quad \rho u_\alpha = \sum_i c_{i\alpha} f_i = \sum_i c_{i\alpha} g_i \tag{35}$$

but higher-order moments are a priori more difficult to compute, since

$$\sum_i c_{i\alpha} c_{i\beta} g_i = \sum_i c_{i\alpha} c_{i\beta} f_i - \frac{\Delta t}{2} \sum_i c_{i\alpha} c_{i\beta} \Omega_i \neq \sum_i c_{i\alpha} c_{i\beta} f_i \tag{36}$$

showing that a collision-kernel-dependent formula must be developed to recover higher-order moments from the g_i, e.g. for the second order moment associated to the viscous stresses.

2.4 Single Relaxation Time (SRT) collision models

We now address the expression for the collision model Ω_i, which was fully general in previous developments. The present discussion will be restricted to collision models that are based on a near-equilibrium approximation, meaning that the collision effect is to relax the solution towards its equilibrium state.

Therefore, in practice, the collision term is expressed as a relaxation term, which includes one or more characteristic relaxation times. Most existing LBM for hydrodynamics rely on a single relaxation time (SRT) approximation, leading to

$$\Omega_i = -\frac{1}{\tau}(f_i - f_i^{eq}) = -\frac{1}{\tau} f_i^{neq} \tag{37}$$

where the expression of f_i^{eq} remains to be found. The expression of the equilibrium distributions (as functions of the macroscopic variables) is the sole element that differs between the SRT-LBM algorithms. It is worth noting that this general formulation for Ω_i leads to an advection-relaxation equations for the f_i, with linear advection and local non-linear relaxation, which makes very significant differences with the associated macroscopic equations, which exhibit non-linear advection.

Now considering the variables g_i, Eq. (31) leads to

$$g_i^{neq} = \left(1 + \frac{\Delta t}{2\tau}\right) f_i^{neq} \Longrightarrow \Omega_i = -\frac{1}{\tau + \frac{\Delta t}{2}} g_i^{neq} \tag{38}$$

The associated closed version of the discrete evolution equation for g_i, Eq. (34), is then

$$g_i(t+\Delta t, \mathbf{x}) = g_i(t, \mathbf{x} - \mathbf{c}_i\Delta t) - \left(\frac{\Delta t}{\tau + \frac{\Delta t}{2}}\right) g_i^{neq}(t, \mathbf{x} - \mathbf{c}_i\Delta t) \tag{39}$$

which can be recast as

$$g_i(t+\Delta t, \mathbf{x}) = g_i^{eq}(t, \mathbf{x} - \mathbf{c}_i\Delta t) + \left(1 - \frac{\Delta t}{\tau_g}\right) g_i^{neq}(t, \mathbf{x} - \mathbf{c}_i\Delta t) \tag{40}$$

where $\tau_g = \tau + \Delta t/2$. This final expression shows that, for SRT models, the equilibrium part is conserved by the collision process while the non-equilibrium part is relaxed (which is coherent with the concept underlying the splitting of f_i and g_i).

It is worth noting that SRT models induce a general closure for the second-order non-equilibrium moment tensor ($\mathbf{\Pi}^{f^{neq},(2)}_{\alpha\beta}$) that appears in the macroscopic momentum equation (18). First, one can write the SRT-closed version of (11):

$$\frac{\partial \mathbf{\Pi}^{f,(n)}_{\alpha_1\cdots\alpha_n}}{\partial t} + \frac{\partial \mathbf{\Pi}^{f,(n+1)}_{\alpha_1\cdots\alpha_{n+1}}}{\partial x_{\alpha_{n+1}}} = -\frac{1}{\tau}\mathbf{\Pi}^{f^{neq},(n)}_{\alpha_1\cdots\alpha_n}, \quad n = 0, N-1 \tag{41}$$

which leads for $n = 2$ to the following evolution equation:

$$\frac{\partial \mathbf{\Pi}^{f,(2)}_{\alpha\beta}}{\partial t} + \frac{\partial \mathbf{\Pi}^{f,(3)}_{\alpha\beta\gamma}}{\partial x_\gamma} = -\frac{1}{\tau}\mathbf{\Pi}^{f^{neq},(2)}_{\alpha\beta} \tag{42}$$

Then splitting moments appearing in the left-hand-side, one obtains

$$\frac{\partial \mathbf{\Pi}^{f^{eq},(2)}_{\alpha\beta}}{\partial t} + \frac{\partial \mathbf{\Pi}^{f^{neq},(2)}_{\alpha\beta}}{\partial t} + \frac{\partial \mathbf{\Pi}^{f^{eq},(3)}_{\alpha\beta\gamma}}{\partial x_\gamma} + \frac{\partial \mathbf{\Pi}^{f^{neq},(3)}_{\alpha\beta\gamma}}{\partial x_\gamma} = -\frac{1}{\tau}\mathbf{\Pi}^{f^{neq},(2)}_{\alpha\beta} \tag{43}$$

which can be rewritten as follows to obtain the intrinsic definition of the non-equilibrium:

$$\mathbf{\Pi}^{f^{neq},(2)}_{\alpha\beta} = -\tau\frac{\partial \mathbf{\Pi}^{f^{eq},(2)}_{\alpha\beta}}{\partial t} - \tau\frac{\partial \mathbf{\Pi}^{f^{neq},(2)}_{\alpha\beta}}{\partial t} - \tau\frac{\partial \mathbf{\Pi}^{f^{eq},(3)}_{\alpha\beta\gamma}}{\partial x_\gamma} - \tau\frac{\partial \mathbf{\Pi}^{f^{neq},(3)}_{\alpha\beta\gamma}}{\partial x_\gamma} \tag{44}$$

Here, all equilibrium moments are known, since they can be expressed as explicit functions of macroscopic variables. The term $\mathbf{\Pi}^{f^{neq},(3)}_{\alpha\beta\gamma}$ is unknown and must be closed.

One can also see that, in practice, a change in the collision model Ω_i will only acts on the third-order non-equilibrium moment $\mathbf{\Pi}^{f^{neq},(3)}_{\alpha\beta\gamma}$.

The evolution equation (76) can be rewritten in a simpler way. In the case of a SRT collision model, the evolution equation (14b) for f_i^{neq} becomes

$$\frac{\partial f_i^{neq}}{\partial t} + c_{i\alpha}\frac{\partial f_i^{neq}}{\partial x_\alpha} = -\frac{1}{\tau}\left(f_i^{neq} - \Lambda_i\right), \quad \text{with } \Lambda_i = -\tau\left(\frac{\partial f_i^{eq}}{\partial t} + c_{i\alpha}\frac{\partial f_i^{eq}}{\partial x_\alpha}\right) \tag{45}$$

which shows that f_i^{neq} relaxes towards Λ_i with the characteristic time τ. Taking the second-order moment, one obtains the following evolution equation for the stresses

$$\frac{\partial \mathbf{\Pi}^{f^{neq},(2)}_{\alpha\beta}}{\partial t} + \frac{\partial \mathbf{\Pi}^{f^{neq},(3)}_{\alpha\beta\gamma}}{\partial x_\gamma} = -\frac{1}{\tau}\left(\mathbf{\Pi}^{f^{neq},(2)}_{\alpha\beta} - \mathbf{\Pi}^{\Lambda,(2)}_{\alpha\beta}\right). \tag{46}$$

This relation is intrinsic to the SRT model, and it shows how the stresses evolves in LBM, even if it is not explicitly solved.

It is worth noting that since $\mathbf{\Pi}^{f^{neq},(3)}_{\alpha\beta\gamma}$ is a high-order term, a low-rank lattice will not enable a good evaluation of it because of quadrature errors, leading to the fact that it is not an independent variable and that it can be expressed as a combination a lower-order moments on this lattice. This results in a kind of numerical-error-induced closure induced by an aliasing-like phenomenon. To account for this phenomena, $\mathbf{\Pi}^{f^{neq},(3)}_{\alpha\beta\gamma}$ should be replaced by $(\mathbf{\Pi}^{f^{neq},(3)}_{\alpha\beta\gamma} - \mathbf{\Upsilon}^{f^{neq},(3)}_{\alpha\beta\gamma})$ in the above formulas.

Let us illustrate this in the case of the athermal low-Mach number approximation for hydrodynamics. After some algebra, using relations (16) and (18), one obtains

$$
\begin{aligned}
-\mathbf{\Pi}_{\alpha\beta}^{f^{neq},(2)} &= \tau\rho c_s^2\left(\frac{\partial u_\alpha}{\partial x_\beta}+\frac{\partial u_\beta}{\partial x_\alpha}-\delta_{\alpha\beta}\frac{2}{3}\frac{\partial u_\gamma}{\partial x_\gamma}\right) \\
&+\tau\left(\frac{\partial \mathbf{\Pi}_{\alpha\beta}^{f^{neq},(2)}}{\partial t}+\frac{\partial \mathbf{\Pi}_{\alpha\beta\gamma}^{f^{neq},(3)}}{\partial x_\gamma}\right)-\tau\left(u_\alpha\frac{\partial \mathbf{\Pi}_{\alpha\gamma}^{f^{neq},(2)}}{\partial x_\gamma}+u_\beta\frac{\partial \mathbf{\Pi}_{\alpha\gamma}^{f^{neq},(2)}}{\partial x_\gamma}\right)
\end{aligned}
\tag{47}
$$

The first term on the right-hand-side is the Navier–Stokes viscous stress tensor, with a viscosity $\nu=\tau\rho c_s^2$, the rest being an error that depends on both the collision model, the lattice, the Mach number and the Reynolds number. An important result is that consistency is not a priori guaranteed for all published collision models !

2.5 Structure of a generic LBM algorithm

A general form of the implementation of LBM-SRT algorithm is given below.

- **Step 1**: Preparation of the collision step
  - **Compute** macroscopic variables appearing in the expression of $f_i^{eq}(t,\mathbf{x})$, i.e. compute the required moments of $g_i(t,\mathbf{x})$ and combine them adequately
  - **Compute** $f_i^{eq}(t,\mathbf{x})(=g_i^{eq}(t,\mathbf{x}))$ associated to the selected collision model
  - **Compute** $f_i^{neq}(t,\mathbf{x})=(f_i(t,\mathbf{x})-f_i^{eq}(t,\mathbf{x}))$
  - **Compute** $g_i^{neq}(t,\mathbf{x})=\left(1+\frac{\Delta t}{2\tau}\right)f_i^{neq}(t,\mathbf{x})$
- **Step 2: collision step** : compute the post-collision state

$$
g_i^{coll}(\mathbf{x})=g_i^{eq}(t,\mathbf{x})+\left(1-\frac{\Delta t}{\tau_g}\right)g_i^{neq}(t,\mathbf{x}),\quad \tau_g=\tau+\Delta t/2
$$

- **Step 3: streaming step** : compute the updated solution at time $t+\Delta t$

$$
g_i(t+\Delta t,\mathbf{x})=g_i^{coll}(\mathbf{x}-\mathbf{c}_i\Delta t)
$$

- **Step 4 (Optional): post-processing** : compute outputs for your application

3.0 LBM COLLISION MODELS TO SOLVE SOME ELEMENTARY PROBLEMS

The general structure of an LBM algorithm has been discussed in the previous section. We now illustrate the versatility and the generality of this approach by addressing some basic simple scalar problems with increasing complexity.

3.1 Poisson equation

Solving a Poisson equation via LBM has been addressed by several authors, who proposed different LBM algorithms to solve the following scalar equation

$$-\varepsilon\nabla^2\phi = A \tag{48}$$

In the method proposed by [145], one has

$$\sum_i f_i = \phi, \quad f_i^{eq} = \omega_i\phi, \quad H_i = -D\omega_i A \tag{49}$$

where H_i is a forcing term added on the right-hand-side of Eq. (8), and $D > 1$ a free parameter. The associated macroscopic equation is

$$\frac{1}{D}\frac{\partial\phi}{\partial t} = \varepsilon\nabla^2\phi + A, \quad \varepsilon = c_s^2 \tag{50}$$

This equation show that the solution of the original Poisson equation (48) corresponds to the steady-state solution of (50). LBM is then here equivalent to an iterative time-marching method to solve the original elliptic problem.

A variant was proposed in [146], in which

$$\sum_{i=0,N-1} f_i = 0, \phi = \frac{1}{1-\omega_0}\sum_{i=1,N-1} f_i,\ f_i^{eq} = \begin{cases}(\omega_0-1)\phi & i=0\\ \omega_i\phi & i=1,N-1\end{cases}, H_i = -\Delta t D\omega_i A \tag{51}$$

It is worthy noting that in the present case the equilibrium functions contain only the zeroth-order moment of f_i, making it possible to use lattice with reduced number of grid points (referred to as "low-order" lattices, since the associated quadrature will be exact for low-order polynomial functions only). In practice, these two methods have been implemented successfully on D1Q3, D2Q5 and D3Q13 lattices

3.2 Scalar linear advection-diffusion equation

A slightly more complex case is the scalar advection-diffusion equation:

$$\frac{\partial\phi}{\partial t} + \nabla\cdot(\mathbf{u}\phi) = \nu\nabla^2\phi \tag{52}$$

where $\mathbf{u}(t,\mathbf{x})$ is a prescribed velocity field. The equilibrium function must now account for the advection term $(\mathbf{u}\phi)$, leading to

$$\sum_{i=0,N-1} f_i = \phi, \quad f_i^{eq} = \omega_i\phi(t,\mathbf{x})\left(1 + \frac{\mathbf{c}_i\cdot\mathbf{u}}{c_s^2}\right) \tag{53}$$

This simple model has been used on D2Q5 and D2Q9 lattices with success, but it is restricted to first-order accuracy since the associated Equivalent Differential Equation is

$$\frac{\partial\phi}{\partial t} + \nabla\cdot(\mathbf{u}\phi) = \nu\nabla^2\phi + \frac{\nu}{c_s^2}\frac{\partial\phi}{\partial t}(\nabla\cdot(\mathbf{u}\phi)) \tag{54}$$

where the last term in the r.h.s is related to the numerical error. For the case of a constant velocity field, this error term can be rewritten in a simpler way, leading to

$$\frac{\partial \phi}{\partial t} + \nabla \cdot (\mathbf{u}\phi) = \nu \left(1 - \frac{\mathbf{u}\cdot\mathbf{u}}{c_s^2}\right) \nabla^2 \phi \tag{55}$$

showing that the method is unstable when $|\mathbf{u}|$ is larger than the lattice speed of sound c_s.

This scheme can be improved [147] by adding a source term F_i to the r.h.s of Eq. (8), which is designed to balance the leading error term, leading to a gain in accuracy and a real second-order accuracy in both space and time in the present case. It is worth keeping in mind that this strategy is commonly used in classical CFD to derived higher-order scheme for convective problems, e.g. Lax-Wendroff, Fromm and Lerat-Peyret schemes for the advection equation and more complex hyperbolic systems [38]. The correction term reads

$$F_i = \omega_i \frac{\mathbf{c}_i}{c_s^2} \left(1 - \frac{1}{2\tau}\right) \frac{\partial}{\partial t}(\mathbf{u}\phi) \tag{56}$$

In practical implementation, the time derivative is computed by using a Finite Differences scheme on the macroscopic variables.

This method can be further improved (considering both robustness and absolute level of error) by considering the following nonlinear collision model, which is observed to yield better results than the linear one when $\mathbf{u}$ obeys the Navier–Stokes equation:

$$f_i^{eq} = \omega_i \phi(t,\mathbf{x}) \left(1 + \frac{\mathbf{c}_i\cdot\mathbf{u}}{c_s^2} + \frac{1}{2c_s^4} Q_{i\alpha\beta} u_\alpha u_\beta\right), \quad Q_{i\alpha\beta} = \left(c_{i\alpha}c_{i\beta} - c_s^2\delta_{\alpha\beta}\right) \tag{57}$$

along with the adequate correction term

$$F_i = \omega_i \frac{\mathbf{c}_i}{c_s^2} \left(1 - \frac{1}{2\tau}\right) \frac{\phi}{\rho_f} \nabla p_f \tag{58}$$

where ρ_f and p_f denote the density and the pressure of the advecting fluid, respectively.

3.3 Scalar wave equation

We show here how to solve the following wave equation via LBM:

$$\frac{\partial \mathbf{J}}{\partial t} + \nabla \cdot \Pi^{f,(2)} = 0 \tag{59a}$$

$$\frac{\partial p}{\partial t} + \nabla \cdot \mathbf{J} = 0 \tag{59b}$$

which is equivalent to

$$\frac{\partial \mathbf{J}}{\partial t} + c^2 \nabla p = 0 \tag{60a}$$

$$\frac{\partial^2 p}{\partial t^2} - c^2 \nabla p = 0 \tag{60b}$$

where c is the wave phase velocity. To this end, one has to define a set of distribution functions f_i such that

$$\sum_i f_i = p, \quad \sum_i \mathbf{c}_i f_i = \mathbf{J}, \quad \Pi^{f,(2)}_{\alpha\beta} = \sum_i c_{i\alpha} c_{i\beta} f_i = c^2 p \delta_{\alpha\beta} \tag{61}$$

The equilibrium function proposed in [148] for uniform Cartesian grids with a D3Q7 lattice is

$$f_i^{eq} = \begin{cases} p - \left(\frac{5p}{2} - \frac{3c^2 p}{2c_s^2}\right)(1-\omega_0) + \frac{3c^2 p}{2c_s^2}(c^2 - c_s^2) & \text{if } i = 0 \\ \omega_i \left(p + \frac{(\mathbf{c}_i \cdot \mathbf{J})}{c_s^2} + \frac{p}{2c_s^4}(c^2 - c_s^2)(\mathbf{c}_i \cdot \mathbf{c}_i - 3c_s^2)\right) & \text{otherwise} \end{cases} \tag{62}$$

A completely different approach was proposed in [149]. Here, one considers

$$\sum_i f_i = \frac{\partial p}{\partial t}, \sum_i c_{i\alpha} f_i^{eq} = 0, \sum_i c_{i\alpha} c_{i\beta} f_i^{eq} = \lambda p \delta_{\alpha\beta}, \quad \lambda = \frac{c^2}{\Delta t(\tau - 1/2)} \tag{63}$$

along with the following equilibrium functions:

$$f_i^{eq} = \begin{cases} \frac{\partial p}{\partial t} - \frac{\lambda p D}{c^2} & i = 0 \\ -\frac{\lambda p D}{(N-1)c^2} & i = 1, N-1 \end{cases} \tag{64}$$

where D is the spatial dimension. The associated Equivalent Differential Equation obtained via a Taylor expansion is

$$\frac{\partial^2 p}{\partial t^2} - c^2 \nabla^2 p = -2\Delta t^2 \lambda \left(\tau^2 - \tau + \frac{1}{6}\right) \nabla^2 \frac{\partial p}{\partial t} \tag{65}$$

showing that the method achieves second order accuracy in time. The stability depends on the sign of the polynomial in τ on the r.h.s. Physical values of τ are very small for realistic applications, leading to a stable method.

The comparison of the two methods above illustrate the flexibility of LBM. In the first one, the zeroth-order moment of the distribution function is equal to p, while in the second case it is $\partial p/\partial t$, leading to very different expressions for the equilibrium functions and numerical properties. Here, one should keep in mind that there is an infinite number of admissible equilibrium functions to solve the problem, exactly as for the classical methods (Finite Differences, Finite Volumes, Finite Elements ...) one can design and infinite number of numerical methods to solve a given equation.

4.0 COLLISION MODELS FOR CLASSICAL HYDRODYNAMICS

4.1 The Bathnagar-Gross-Krook (BGK) collision model

We now discuss the simplest SRT collision model, namely the Bathnagar-Gross-Krook (BGK) collision model, for which the equilibrium function for athermal low-Mach hydrodynamics is given by

$$f_i^{eq,BGK} = \omega_i \rho \left(1 + \frac{(\mathbf{c}_i \cdot \mathbf{u})}{c_s^2} + \frac{1}{2}\frac{(\mathbf{c}_i \cdot \mathbf{u})^2}{c_s^4} - \frac{1}{2}\frac{(\mathbf{u} \cdot \mathbf{u})}{c_s^2}\right) \tag{66}$$

This expression can be found by performing a Hermite-polynomial expansion of the exact continuous equilibrium function (referred to as the Maxwellian in statistical kinetic theory) on the polynomial basis associated with Cartesian lattices [1, 36]:

$$f_i^{eq,Maxwell} = \rho \left(\frac{1}{2\pi RT} \right) \exp \left(-\frac{(\mathbf{c}_i \cdot \mathbf{u})^2}{2RT} \right) \tag{67}$$

where R and T are the gas constant and the temperature, respectively. It is worth noting that (66) is not the unique possible expression for the equilibrium functions. Some purely synthetic (i.e. not derived from the physical continuous Maxwellian) expressions can be found, that are tuned to fulfil the constraints discussed above dealing with Ω_i and the moments of f_i. A general expression (restricted to quadratic terms, but it can be straightforwardly extended to any order)

$$f_i^{eq,general} = \omega_i \rho \left(a_{i,0} + a_{i,1}(\mathbf{c}_i \cdot \mathbf{u}) + a_{i,2}(\mathbf{c}_i \cdot \mathbf{u})^2 + a_{i,3}(\mathbf{u} \cdot \mathbf{u}) \right) \tag{68}$$

As an example, Yan et al. [150] considered the following formulation :

$$f_i^{eq,Yan} = \begin{cases} \omega_0 \rho \left(B_0 + B_6(\mathbf{u} \cdot \mathbf{u}) \right) & \text{if } i = 0 \\ \omega_i \rho \left(A_0 + A_2(\mathbf{c}_i \cdot \mathbf{u}) + A_5(\mathbf{c}_i \cdot \mathbf{u})^2 + A_6(\mathbf{u} \cdot \mathbf{u}) \right) & \text{otherwise} \end{cases} \tag{69}$$

and found that correct expressions of the arbitrary coefficients $A_0, A_2, A_5, A_6, B_0, B_6$ to recover athermal low-Mach flows in dimension D on a lattice with N points are

$$A_0 = B_0 = \frac{1}{N},\ A_2 = \frac{D}{(N-1)c^2},\ A_5 = \frac{D(D+2)}{2(N-1)c^4},\ A_6 = -\frac{D}{2(N-1)c^2}, B_6 = \frac{1}{c^2} \tag{70}$$

where c denotes $|\mathbf{c}_i|$. The lattice speed of sound is given by

$$c_s^2 = \frac{(N-1)c^2}{ND} \tag{71}$$

Non-polynomial expressions have also been proposed, e.g. in Entropic LBM (see Sect. 4.3.2).

On uniform Cartesian grids, one should use at least the D2Q9 lattice to get reliable solutions in 2D simulations, and D3Q19 or D3Q27 lattices in 3D.

This size of the lattice can be reduced in 2D considering hexagonal cells with a D2Q7 lattice. On a 2D hexagonal grid (on which 1) the discrete velocities and 2) the quadrature coefficients and 3) the polynomial basis are not the same as on the Cartesian grid !), the new expression of the equilibrium function derived from the physical Maxwellian is

$$f_i^{eq,hexa} = \omega_i \rho \left(1 + 4(\mathbf{c}_i \cdot \mathbf{u}) + 8(\mathbf{c}_i \cdot \mathbf{u})^2 - 2(\mathbf{u} \cdot \mathbf{u}) \right) \tag{72}$$

Another formula could be obtained setting $N = 7$ and $D = 2$ in Eq.(69).

4.2 BGK-like model for Streamfunction-Vorticity formulation

A way to minimize the lattice size for 2D incompressible flows is to consider the Streamfunction-Vorticity ($\psi - \Omega$) formulation of the incompressible Navier–Stokes equations [151, 152]:

$$\frac{\partial \Omega}{\partial t} + \frac{\partial}{\partial x}\left(u\Omega\right) + \frac{\partial}{\partial y}\left(v\Omega\right) = \nu\left(\frac{\partial^2 \Omega}{\partial x^2} + \frac{\partial^2 \Omega}{\partial x^2}\right), \tag{73a}$$

$$\left(\frac{\partial^2 \psi}{\partial x^2} + \frac{\partial^2 \psi}{\partial x^2}\right) = -\Omega \tag{73b}$$

Here the transport equations for Ω is a linear advection-diffusion equation, that can be solved on a D2Q5 Cartesian lattice, while the equation for ψ is a scalar Poisson equation, which can also be solved on the same D2Q5 lattice (see Section 3.0). Since there are two different variables obeying different equations, it is convenient to define one set of distribution functions and an associated equilibrium function for each variable, leading to a Double Distribution Function (DDF) method:

- For the vorticity:

$$\sum_{i=0,4} f_i^{\Omega} = \Omega, \quad f_i^{\Omega,eq} = \omega_i \Omega \left(1 + \frac{(\mathbf{c}_i \cdot \mathbf{u})}{c_s^2}\right) \tag{74}$$

- For the Streamfunction:

$$\sum_{i=0,4} f_i^{\psi} = \psi, \quad f_i^{\psi,eq} = \omega_i \psi \tag{75}$$

Using this approach, one 1) decreases the size of the stencil and 2) simplifies the expressions of the equilibrium functions by decreasing their polynomial order but) increases the total number of distribution functions with respect to D2Q9 LBM based on the conservative formulation of the Navier–Stokes equations. The reduced nonlinearity leads to select this formulation for implementation using Quantum Algorithms by Budinski [152].

4.3 More efficient collision models for hydrodynamics

The BGK-SRT models discussed in the preceding sections are observed to lack robustness in complex flows, e.g. high-Reynolds turbulent flows in complex geometries. To cure this problem, several ways to improve robustness while preserving the SRT approach have been recently proposed. As a matter of fact, derivation of robust LBM with controlled dissipation is a very active field of reasearch (in the same way as numerical schemes for convective terms for Euler and Navier–Stokes equations).

As discussed above, changing the collision model amounts to change the definition of f_i^{eq} to get a better control of $\mathbf{\Pi}_{\alpha\beta}^{f^{neq},(2)}$, i.e. the viscous stresses and higher-order terms, while still enforcing definitions (16). In practice, this amounts to modify $\mathbf{\Pi}_{\alpha\beta\gamma}^{f^{neq},(3)}$ (and $\mathbf{\Upsilon}_{\alpha\beta\gamma}^{f^{neq},(3)}$ if the lattice has no enough point to compute exactly the related integral). This amounts to close the constitutive equation for the stress tensor, and one can make an analogy with physics of non-Newtonian fluids. This point is made clear rewriting the evolution equation (76) for $\mathbf{\Pi}_{\alpha\beta}^{f^{neq},(2)}$ as

$$\frac{\partial \mathbf{\Pi}_{\alpha\beta}^{f^{neq},(2)}}{\partial t} + \frac{\partial \mathbf{\Pi}_{\alpha\beta\gamma}^{f^{neq},(3)}}{\partial x_\gamma} - \left(u_\alpha \frac{\partial \mathbf{\Pi}_{\beta\gamma}^{f^{neq},(2)}}{\partial x_\gamma} + u_\beta \frac{\partial \mathbf{\Pi}_{\alpha\gamma}^{f^{neq},(2)}}{\partial x_\gamma}\right) = -\frac{1}{\tau}\left(\mathbf{\Pi}_{\alpha\beta}^{f^{neq},(2)} + S_{\alpha\beta}\right) \tag{76}$$

in which moments of f_i^{eq} have been replaced by their expressions as functions of density and velocity. It is seen that $\mathbf{\Pi}_{\alpha\beta\gamma}^{f^{neq},(3)}$ is the only tunable parameter, since $S_{\alpha\beta}$ denotes the exact physical viscous stress tensor. The quadrature error $\mathbf{\Upsilon}_{\alpha\beta\gamma}^{f^{neq},(3)}$ may be added for the sake of completeness.

For the classical BGK-SRT model (66) their is no explicit closure: $\mathbf{\Pi}_{\alpha\beta\gamma}^{f^{neq},(3)}$ originates in quadrature errors and higher-order moments equations. Therefore, there is no explicit control on the committed error and related numerical stability issues.

Two popular stabilizing approaches are presented below, which illustrate very different and powerful approaches.

4.3.1 Regularized collision models

The key idea underlying regularized collision models is to remove the contribution of $\mathbf{\Pi}_{\alpha\beta\gamma}^{f^{neq},(3)}$ and higher-order moments [125, 126, 153–160]. To implement this, it is worth noting that, combining the definition of f_i^{eq} with Eq. (37) and relations (17), one can formally expand the non-equilibrium components of f_i and g_i as functions of moments of order greater or equal than 2, yielding

$$f_i^{neq} = \omega_i \sum_{p\geq 2} \mathbf{a}_p \mathbf{\Pi}^{f^{neq},(p)}, \quad g_i^{neq} = \omega_i \sum_{p\geq 2} \mathbf{b}_p \mathbf{\Pi}^{g^{neq},(p)} \tag{77}$$

where $\mathbf{a}_p$ and $\mathbf{b}_p$ are real square matrices of rank p. Their expression is not given here for the sake of brevity, but it is worth noting that they are lattice-dependent. Here arise a classical problem in numerical analysis, i.e. finding the best low-order polynomial (with fixed order) that leads to the best fit for a given function on a selected interval.

The Projective Regularization consists of simply truncating the expansion to the second order, leading to

$$g_i^{neq,PR} = \omega_i \mathbf{b}_2 \mathbf{\Pi}^{g^{neq},(2)}, \quad \mathbf{\Pi}_{\alpha\beta}^{g^{neq},(2)} = \sum_{i=0,N-1} c_{i\alpha} c_{i\beta} (g_i - g_i^{eq}) \tag{78}$$

The Recursive Regularization proposed by Malaspinas is based on a more complex approach, which is based on recursive relations that exist between Hermite polynomials (the f_i being expanded on a Hermite polynomial basis). The closure is expressed as

$$\mathbf{\Pi}_{\alpha\beta\gamma}^{g^{neq},(3),RR} = u_\alpha \mathbf{\Pi}_{\beta\gamma}^{g^{neq},(2)} + u_\beta \mathbf{\Pi}_{\gamma\alpha}^{g^{neq},(2)} + u_\gamma \mathbf{\Pi}_{\alpha\beta}^{g^{neq},(2)} \tag{79}$$

leading to

$$g_i^{neq,RR} = \omega_i \left(\mathbf{b}_2 \mathbf{\Pi}^{g^{neq},(2)} + \mathbf{b}_3 \mathbf{\Pi}^{g^{neq},(3),RR} \right) \tag{80}$$

A more recent version [158], referred to as Hybrid Recursive Regularization consists of hydridizing the LBM stress tensor with a Finite Difference-based evaluation of the viscous stress tensor (denoted $S_{\alpha\beta}^{FD}$):

$$g_i^{neq,HRR} = \omega_i \mathbf{b}_2 \mathbf{\Pi}^{g^{neq},(2),HRR}, \quad \mathbf{\Pi}_{\alpha\beta}^{g^{neq},(2),HRR} = \sigma \sum_{i=0,N-1} c_{i\alpha} c_{i\beta} (g_i - g_i^{eq}) - (1-\sigma) S_{\alpha\beta}^{FD} \tag{81}$$

These modified expressions of g_i^{neq} are used during the collision step are are computed during the reconstruction step (see Section 2.5). Let us mention that regularized models are very powerful, since they lead to

robust simulations with controlled dissipation. From the theoretical point of view, it can be shown that they mostly damp non-physical numerical modes (see Section 5.2). They are used in the PowerFlow and ProLB commercial LBM softwares and in the Palabos open source code. Regularized collision models have also proven their efficiency in more complex cases: compressible flows, multiphase flows, combustion ...

The previous developments are based on the raw moments $\Pi^{f,(n)}$ which are computed using the discrete velocities $\mathbf{c}_i$. Improved collision models can also be obtained replacing the later by Hermite polynomials of $\mathbf{c}_i$ (Hermite moments), by centred velocities $(\mathbf{c}_i - \mathbf{u})$ [161–164] and even Hermite polynomials of centered velocities. Moments can also be replaced by cumulants [165–168]. In all cases, one tries to find a truncated expansion of the equilibrium function that leads to a more efficient (robustness, accuracy, numerical efficiency) closure for unknown high-order moments. Since we are truncating an infinite series expansion, an aliasing-like phenomena occurs, which can corrupt the computed moments. To prevent or minimize this aliasing, the commonly shared idea is to find a basis in which it will be naturally weak. An ideal basis would be an orthogonal basis: in this case, the truncated expansion is the best approximation on the subspace on which the truncation is performed. This formal change in the expansion yield new expressions for the equilibrium functions f_i^{eq} and then define implicitly new non-equilibrium functions. As a consequence, the closure for $\mathbf{\Pi}_{\alpha\beta\gamma}^{f^{neq},(3)}$ automatically change. The reader is referred to [169] for an exhaustive and comprehensive analysis of the links between different expansions.

It is worth noting that changing the statistical quantities used to expand the collision kernel don't just amount to apply a linear transformation: as a matter of fact, there exist some nonlinear relations between them. As an example, the n-th order cumulant κ_n is related to the raw moments m_i by the following general relation:

$$\kappa_n = m_n - \sum_{k=1,n-1} \binom{n-1}{k-1} \kappa_k m_{n-k} \tag{82}$$

showing that the n-th order raw moment is a polynomial function of degree n of the first n cumulants:

$$m_1 = \kappa_1 \tag{83a}$$
$$m_2 = \kappa_2 + \kappa_1^2 \tag{83b}$$
$$m_3 = \kappa_3 + 3\kappa_2\kappa_1 + \kappa_1^3 \tag{83c}$$
$$m_4 = \kappa_4 + 4\kappa_3\kappa_1 + 3\kappa_2^2 + 6\kappa_2\kappa_1^2 + \kappa_1^4 \tag{83d}$$

The centered moments μ_i are revovered taking $\kappa_1 = m_1 = 0$:

$$\mu_1 = 0 \tag{84a}$$
$$\mu_2 = \kappa_2 \tag{84b}$$
$$\mu_3 = \kappa_3 \tag{84c}$$
$$\mu_4 = \kappa_4 + 3\kappa_2^2 \tag{84d}$$

The centered moments and the raw moments can be obtained from each other using the following formula:

$$\mu_r = \sum_{i=0,r} \binom{i}{r} m_{r-i}(-m_1)^i = \sum_{i=0,r} \binom{i}{r} m_i(-m_1)^{r-i}, \quad m_r = \sum_{i=0,r} \binom{i}{r} \mu_{r-i}\mu^i = \sum_{i=0,r} \binom{i}{r} \mu_i\mu^{r-i} \tag{85}$$

where μ denotes the mean value, leading to

$$m_2 = \mu_2 + \mu^2 \tag{86a}$$
$$m_3 = \mu_3 + 3\mu_2\mu + \mu^3 \tag{86b}$$
$$m_4 = \mu_4 + 4\mu_3\mu + 6\mu_2\mu^2 + \mu^4 \tag{86c}$$
$$\tag{86d}$$

along with

$$\mu_0 = 1 \tag{87a}$$
$$\mu_1 = 0 \tag{87b}$$
$$\mu_2 = m_2 - m_1^2 \tag{87c}$$
$$\mu_3 = m_3 - 3m_2m_1 + 2m_1^3 \tag{87d}$$
$$\mu_4 = m_4 - 4m_3m_1 + 6m_2m_1^2 - 3m_1^4 \tag{87e}$$

This approach was also extended to the case of Multiple Relaxation Time LBM, e.g. the Cascaded LBM proposed by Geier [161, 164], which relies on a recursive orthogonalization procedure of the moments (some kind of Gramm-Schmidt method for the moments), which can be understood as the search for an orthogonal-function-based approximation of the non-truncated expansion of the non-equilibrium functions. This procedure amounts to defining new expressions for the equilibrium functions [170].

4.3.2 Entropic models

Enforcing stability in LBM is a non-trivial task, as for classical macroscopic numerical methods. But it is worth noting that the LBM framework is less friendly, since the viscosity is not explicitly appearing in governing equations, and that an additional step is needed to get equivalent macroscopic equations in which the effect of leading error terms can be interpreted in a classical way (see Section 5.0).

Therefore, the idea of enforcing an additional constraint to improve stability is appealing [171, 172](this is the field of *structure-preserving methods* [40]). This approach is well illustrated by the concept of entropic numerical schemes for shock-capturing when solving the Euler equations: numerical schemes are designed in order to satisfy a discrete entropy constraint to prevent the occurence of spurious wiggles near discontinuities. This idea has been used in the LBM framework to derive stabilized collision models: since wiggles are unphysical, they violate the second law of thermodynamics (i.e. they don't obey Boltzmann's H-theorem), leading to the entropic derivation of LBM schemes pioneered by Karlin, Ansumali and colleagues in the late 1990s and early 2000s [173–186]. In such a scheme, the collision model is designed such that the discrete equation obeys a built-in H-theorem.

A first difficulty originates in the fact that the classical statistical definition entropy function associated to the continuous Boltzmann equation (and kinetic theory) does not hold in the discrete case. Therefore, a new synthetic definition must be found. Second, a way to enforce the associated discrete pseudo-H-theorem must be found.

Most existing works dealing with entropic LBM use the following discrete entropy function $H(f_0, ..., f_{N-1}; \omega_0, ..., \omega_{N-1})$:

$$H(f_0, ..., f_{N-1}; \omega_0, ..., \omega_{N-1}) = \sum_{i=1,N-1} f_i \ln\left(\frac{f_i}{\omega_i}\right) \tag{88}$$

The expression of the equilibrium functions that minimize this discrete entropy in dimension D (while still enforcing relations (16) and (19)) in the athermal case is

$$f_i^{eq} = \omega_i \rho \Pi_{\alpha=1,D} \left(2 - \sqrt{1+{u'_\alpha}^2}\right) \left(\frac{\frac{2}{\sqrt{3}} u'_\alpha + \sqrt{1+{u'_\alpha}^2}}{1 - u'_\alpha/\sqrt{3}} \right)^{c_{i\alpha}/\sqrt{3}c_s} \quad , \quad u'_\alpha = u_\alpha / c_s \tag{89}$$

which is a very illustration of the fact that non-polynomial expressions of the equilibrium function may be used. It is important noting this expression doesn't hold for thermal flows, for which more complex formulations exist. The collision step is essentially a relaxation step toward f_i^{eq}. Since the macroscopic quantities are left unchanged by the collision, the entropy H should also be kept constant (according to the definition of the local equilibrium and to the fact that an extremum of H is sought for). In order to find the correct relaxation parameter β, one must solve the following problem:

$$\text{find } \beta \text{ such that} \quad H(\mathbf{f}) = H(\mathbf{f} + \beta(\mathbf{f}^{eq} - \mathbf{f})) \tag{90}$$

In practice, the optimal value of β is found by solving this nonlinear problem by a Newton-type iterative procedure at each grid point and each time step. In order to decrease the computational cost, some approximate fixed values can be used but the exact enforcement of the entropy constraint is no longer guaranteed. Once β is computed, the time step Δt is replaced by $\beta \Delta t$.

This approach leads to very robust LBM schemes. Like regularized models, it has been extended to many cases, e.g. multiphase flows and compressible flows. Some Essentially Entropic LBM schemes with reduced computational cost have been proposed [187], with a weaker entropy constraints that does not totally preclude wiggles (in the same way that ENO schemes for Euler equations are not strictly wiggle-free).

4.4 More physics on same lattices: segregated methods

It has been seen above that the number of points in a lattice governs the maximum order of the moments of f_i that can be accurately captured. Increasing the maximum degree of the moments that must be captured, one has to face the following problems if the procedure described above is strictly followed:

- **Curse of nonlinearity**: increasing the maximum degree, one must increase the order of truncation in the expansion of the equilibrium functions f_i^{eq}. Therefore the collision model nonlinearity is increased.
- **Curse of dimensionality**: increasing the maximum degree of the physical moments, one must increase the order of the quadrature in the velocity space used to compute them. Therefore, the number of discrete velocities $\mathbf{c}_i$ and distribution function f_i is increased.
- **Curse of complexity**: Each f_i being a computational unknown, one must solve one evolution equation per discrete velocity. Therefore the curse of dimensionality also leads to an increase in the complexity, since more equations must be solved.

This is illustrated by the cas of hydrodynamic equations. In 3D, athermal low-Mach Navier-Stokes equations are recovered using SRT-BGK with a quadratic equilibrium function on a D3Q27 lattice, while a quartic equilibrium function on a D3Q137 lattice is required to recover the compressible Navier-Stokes equations. This illustrate the fact that increasing the maximum degree of physically captured moment by 1 (here, one adds the energy equation to the mass and momentum equations to capture compressibility effects) one increases the

computational cost of the method in a very significant way. The same phenomena appears when switching from a Newtonian fluid to a non-Newtonian fluid for which stresses must be computed solving adequate evolution equations.

In order to avoid the definition of LBM schemes that would be too expensive to be used for practical applications, some techniques have been developed to prevent the complexity explosion. The underlying idea is based on the observation that the problem comes from the highest-order moment, which governs the size of the full method. To overcome this issue, segregated methods in which the highest-order moment (energy for compressible or thermal flows, stresses for non-Newtonian fluids ...) is treated in a separate way from other moments. This way, the other moments may (at least theoretically) be computed on the same lattice as the one required to solve the problem without this highest-order moment. In practice, this means that one will try to solve compressible LBM problem on the same lattice as for the athermal nearly-compressible LBM. Here, dimensionality and complexity are now under control.

Two main families of segregated methods have been proposed:

- **Multiple Distribution Functions** : a new set of distribution functions (with associated collision model) are introduced to compute the evolution of the highest-order moment. In the case of compressible thermal flows, one introduces a set h_i such that $\sum_i h_i = T$ (for temperature) or $\sum_i h_i = \rho E$, while still having $\sum_i f_i = \rho$ and $\sum_i c_{i\alpha} f_i = \rho u_\alpha$. The main problems here are i) to develop the collision model for the h_i, i.e. finding h_i^{eq} and ii) coupling the two sets f_i and h_i. The case of extension to thermal and/or compressible flows has been addressed in many papers, among which [66, 67]. Another example is provided in [188], in which an LBM with three sets of distribution functions is developed to simulate three-phase non-Newtonian flows. Last examples mentioned here are the two-distribution-function sets used in [108] for magnetohydrodynamics, with one set for hydrodynamic mass and momentum equations and a second one for the magnetic induction equation, and the four-distribution-function sets method of Mendoza and Munoz [99] for three-dimensional electrodynamics.

- **Hybrid Methods** : the macroscopic equation for the highest-order moment is solved in a classical way via Finite Difference, Finite Volume, Finite Element or another method. This approach was introduced in [41] for thermal flows. The main identified problems are i) to discretize the new equation in an efficient way and ii) to enforce the discrete compatibility between the LBM part and the macroscopic equations. The later problem originates in the fact that the highest-order moments appears as the flux of the preceding one (see Eq. 11). Therefore some discrete compatibility issues arise if no specific care is taken when discretizing the macroscopic equations. This approach is illustrated for compressible flows in several papers, among which [42, 44–46, 71**?**]. As an example, this may lead to some conservativity and stability problems when addressing compressible flows [70, 81], a problem that can be solved as demonstrated very recently [43]. Similar approaches were used in [189–191] for viscoelastic fluids, in which mass and momentum equations are solved using LBM while macroscopic constitutive equations for stresses are solved using Finite Difference or Finite Volume Methods. Another example is the hyrbid method developed in [60, 63, 192] to account for humid air equation of state, in which the prognostic equations for water phase mass fractions are solved using a Finite Difference method.

5.0 NUMERICAL ANALYSIS OF SRT-BGK MODEL FOR NEARLY-INCOMPRESSIBLE HYDRODYNAMICS

We now briefly survey the numerical analysis of LBM. It must be kept in mind that very complicated collision models escape detailed theoretical analysis. Therefore, the discussion below will be mostly restricted to the

SRT-BGK scheme.

5.1 Order of accuracy and Equivalent Differential Equation

A classical way to characterize a numerical scheme is to derive its Equivalent Differential Equation performing a Taylor series expansion. This approach has been addressed by several authors, e.g [193–195], but the first complete analysis of the SRT-BGK was performed very recently [127, 129]. The work by Wissocq [127] is used in the present section, and the reader is referred to it for details. The starting point is the streaming step presented in Section 2.5, which can be rewritten as follows for the sake of simplicity

$$g_i(t+\Delta t, \mathbf{x}+\mathbf{c}_i\Delta t) = g_i^{coll}(t,\mathbf{x}) \tag{91}$$

where $g_i^{coll}(t,\mathbf{x})$ is the result of the collision step. Before carrying out the Taylor expansion, it is useful to non-dimensionalize this equation. The reason for that is that there are two small parameters in the full expansion, and that non-dimensional expressions render the comparison between the amplitudes of the error terms easier.

Introducing a reference length $\ell = 1/k$ (where k is the associated wavenumber), one obtains the following dimensionless quantities (denoted by an asterisk)

$$t^* = \frac{kct}{c_s}, \quad x_\alpha^* = kx_\alpha = \frac{x_\alpha}{\ell}, \quad \text{and} \quad \mathbf{c}_i^* = \mathbf{c}_i\frac{c_s}{c},\ c = \frac{c_s\Delta x}{\Delta t} \tag{92}$$

It is worth noting that the components of the dimensionless vectors $\mathbf{c}_i^*$ exhibit integer values. The streaming step can be rewritten as

$$g_i\left(t^* + \varepsilon\frac{\Delta t}{\tau}, \mathbf{x}^* + \varepsilon\frac{\Delta t}{\tau}\mathbf{c}_i^*\right) = g_i^{coll}(t^*,\mathbf{x}^*), \quad \varepsilon = \frac{k\tau c}{c_s} = \frac{\tau c}{\ell c_s} \tag{93}$$

The small parameter ε is interpreted as being the Knudsen number Kn in classical hydrodynamics. In this case, the mean free path of fluid particules is very small compared to the analysis scale, yielding $\varepsilon = Kn \ll 1$. The second parameter arising here is $\Delta t/\tau$, i.e. the ratio of the numerical time step to the relaxation time.

Expanding the right-hand side of (93), one obtain after some algebra (space and time coordinates are not denoted for the sake of clarity since all terms are taken at the same time and same location)

$$D_i g_i = -\frac{\tau}{\Delta t}\frac{1}{\varepsilon}(g_i - g_i^{coll}) - \sum_{n\geq 2}\frac{\varepsilon^{n-1}}{n!}\left(\frac{\Delta t}{\tau}\right)^{n-1} D_i^n g_i \tag{94}$$

where D_i is the advection operator:

$$D_i = \left(\frac{\partial}{\partial t^*} + c_{i\alpha}^*\frac{\partial}{\partial x_\alpha^*}\right) \tag{95}$$

After some (tedious and cumbersome) algebra, this expression can be recast in the following final formulation for the Equivalent Differential Equation related to f_i

$$D_i f_i = -\frac{1}{\varepsilon}(f_i - f_i^{eq}) + \frac{\varepsilon^2}{12}\left(\frac{\Delta t}{\tau}\right)^2 D_i^3 f_i - \frac{\varepsilon^4}{5!}\left(\frac{\Delta t}{\tau}\right)^4 D_i^5 f_i + \sum_{p\geq 3}\frac{c_{2p+1}}{(2p+1)!}\varepsilon^{2p}\left(\frac{\Delta t}{\tau}\right)^{2p} D_i^{2p+1} f_i \tag{96}$$

where the coefficients c_n are given by

$$c_0 = 2, \quad c_n = -\sum_{k=0} n \begin{pmatrix} n \\ k \end{pmatrix} c_k = 2\frac{G_{n+1}}{n+1},\ n \geq 1 \tag{97}$$

where G_n is the n-th Genocchi number.

A first comment is that the leading error term is O(Δt^2), leading to the fact that the SRT-BGK method is second-order accurate in both space and time. It can also be seen that only odd power of the advection operator D_i arise in the error term, meaning that only dispersive numerical error is expected, explaining why this method exhibit very low spurious dissipation, making it very efficient for simulation of long-time propagation.

As a matter of fact, this analysis can be further refined by reminding that

$$f_i = f_i^{eq} - \varepsilon D_i f_i^{eq} + O(\varepsilon^2) \tag{98}$$

leading to

$$\frac{\varepsilon^2}{12}\left(\frac{\Delta t}{\tau}\right)^2 D_i^3 f_i = \frac{\varepsilon^2}{12}\left(\frac{\Delta t}{\tau}\right)^2 D_i^3 f_i^{eq} - \frac{\varepsilon^3}{12}\left(\frac{\Delta t}{\tau}\right)^2 D_i^4 f_i^{eq} + O(\varepsilon^4) \tag{99}$$

This new expression exhibits the operator $D_i^4 f_i^{eq}$ which corresponds to an hyperviscosity term. As a consequence, a small amounts of numerical dissipation may be expected, mainly concentrated at small scales. The associated error terms arising in the macroscopic equations will not be discussed here, since their analysis is a very heavy task (see [127] for some detailed expressions on 1D and 2D lattices).

5.2 Von Neumann-like Linearized Spectral Analysis and modal decomposition

Being a numerical method, LBM can be analyzed using the Linearized Spectral Analysis which allows for 1) the identification of numerical modes that underly the computed solution and to 2) measure the numerical dispersion and the numerical dissipation experienced by each mode at a given wavenumber k. This kind of analysis has been applied to LBM since the mid-1990s, and many schemes have been scrutinized this way, e.g. [56, 196–201]. A recent an important new step for LSA of LBM was done by Wissocq et al. [202], who bridge between the analysis of the numerical modes related to the distribution functions f_i and those of the macroscopic quantities.

Following the classical steps of the von Neumann analysis, one first define a steady uniform base flow $(\bar{\rho}, \bar{u})$ which is associated to base distribution functions $\bar{f}_i = f_i^{eq}(\bar{\rho}, \bar{u})$. The perturbation field is then

$$f_i' = f_i - \bar{f}_i \tag{100}$$

and the post-collision state can be expanded, leading to

$$f_i^{coll}(f_j) = f_i^{coll}(\bar{f}_j) + \left.\frac{\partial f_i^{coll}}{\partial f_j}\right|_{f_j=\bar{f}_j} f_j' + O(f_j'^2) \tag{101}$$

The streaming step for the fluctuating field is

$$f_i'(\mathbf{x} + \mathbf{c}_i\Delta t, t + \Delta t) = \left.\frac{\partial f_i^{coll}}{\partial f_j}\right|_{f_j=\bar{f}_j} f_j'(\mathbf{x}, t) \tag{102}$$

The next step consists of considering plane monochromatic wave fluctuations:

$$f_i'(\mathbf{x},t) = \hat{f}_i \exp(\mathrm{i}(\mathbf{k}\cdot\mathbf{x} - \omega t)) \tag{103}$$

where $\hat{f}_i \in \mathbb{C}, \mathbf{k}$ and $\omega = (\omega_r + \mathrm{i}\,\omega_\mathrm{i}) \in \mathbb{C}$ are the complex tiamplitude, the wavenumber and the complex frequency, respectively. It is reminded here that ω_r is related to the velocity of the wave, since the group velocity v_g and the phase velocity v_ϕ are given by

$$v_\phi = \frac{\omega_r}{\|\mathbf{k}\|}, \quad v_g = \frac{\partial \omega_r}{\partial \|\mathbf{k}\|} \tag{104}$$

Introducing the amplitude vector $\hat{\mathbf{F}} = (\hat{f}_0, \cdots, \hat{f}_{N-1})^T$ and inserting (103) into (102), one obtains a generalized eigenvalue problem:

$$e^{-\mathrm{i}\omega}\hat{\mathbf{F}} = \mathbf{M}\hat{\mathbf{F}} \tag{105}$$

where the $N \times N$ matrix $\mathbf{M}$ depends on the collision model. On a lattice with N points/discrete velocities/distribution functions, one has N eigenvectors and N complex frequencies, which are wave-number-dependent. While the analysis of ω_r and ω_i is commonly performed to study numerical stability and dispersive errors, eigenvectors are usually not discussed.

Wissocq has recently shown that these eigenvectors carry a very interesting informations dealing with physical macroscopic fluctuations. Reminding that an eigenvector of $\mathbf{M}$ is a vector of size N whose components are the complex amplitudes of distribution function fluctuations, one can reconstruct fluctuations of density, ρ', and momentum, $(\rho\mathbf{u})'$ using in linear combinations of these eigenvectors.

Computing the moments of a single eigenvector, one can evaluate the macroscopic information associated to it. Keeping in mind the fact that macroscopic fluctuations can be decomposed as the sum of three physical waves (namely upstream travelling acoustic wave, dowstream travelling acoustic wave and vorticity wave according to the Kovasznay decomposition in the present athermal case, see [203] for an exhaustive discussion of this decomposition and its weakly nonlinear extension), one can compute the part of each physical wave associated to each eigenvectors. On the ground of this decomposition, numerical modes (a mode being associated to an eigenvector) can be classified into 3 groups:

- **Observable physical modes**: modes that carry non-zero fluctuations of macroscopic quantities which correspond to a physical wave, i.e. $(\rho', (\rho\mathbf{u})') \neq (0, \mathbf{0})$ with acoustic or vortical fluctuations
- **Observable unphysical modes**: modes that carry non-zero fluctuations of macroscopic quantities which don't correspond to a physical wave, i.e. $(\rho', (\rho\mathbf{u})') \neq (0, \mathbf{0})$ with non-acoustic and non-vortical fluctuations
- **Non-observable modes**: modes that carry no macroscopic information, i.e. $(\rho', (\rho\mathbf{u})') = (0, \mathbf{0})$

Typical results are shown below, see Figs.11 to 13. The analysis of the basic SRT-BGK scheme is displayed in Fig. 11 for different values of the uniform base flow speed. The main observations are that i) the propagation speeds of the three captured physical modes is well predicted up to $k\Delta x \simeq \pi/2$, ii) the vorticity mode is beared by three numerical modes and is captured at all wavenumbers, iii) the two acoustic modes are not represented at high wavenumbers and iv) some components of the vorticity modes travel at unphysical speed at high wavenumbers v) the numerical viscosity is negligible at all physically captured wavenumber on all physical modes. The later feature explains why LBM is very efficient for wave propagation problems.

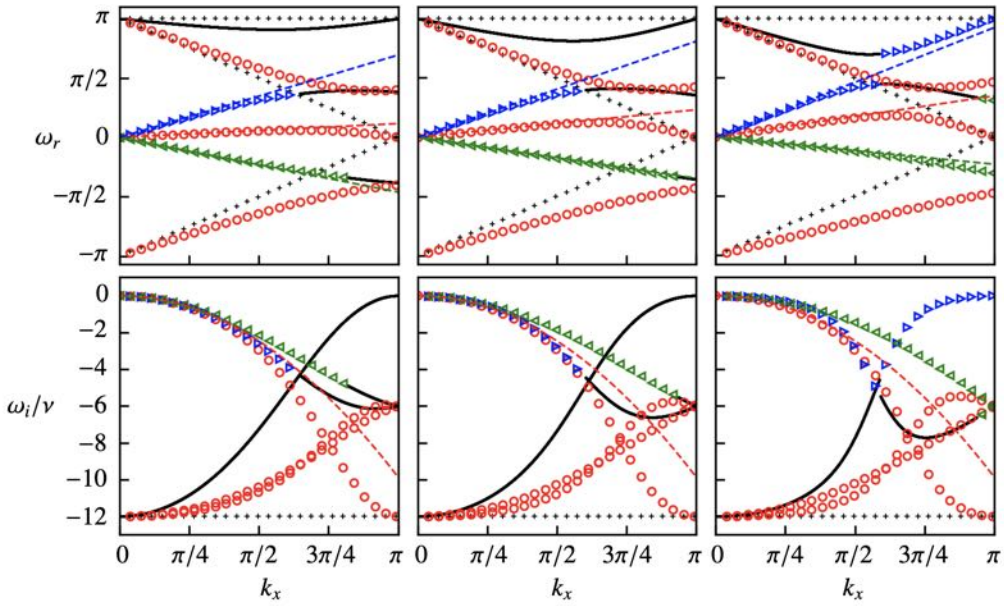

Figure 11: Linearized Stability Analysis of the SRT-BGK scheme on the D2Q9 lattice for different values of the base flow speed U_0 (left: $U_0/c_s = 0.2$, middle: $U_0/c_s = 0.4$, right: $U_0/c_s = 0.6$). Top: phase speed of the 9 numerical modes. Bottom: numerical viscosity normalized by the physical viscosity. Symbols denote observable physical modes at a given normalized wavenumber $k\Delta x$; Green triangles: upstream travelling acoustic mode, Blue triangles: downstream travelling acoustic mode, Red squares: vorticity mode, thick solid line: observable unphysical modes, crosses: non-observable modes. From [200].

Results of the same analysis are displayed in Figure 12 for the PR and RR regularized scheme. Those associated to the Hybrid Recursive Regularized scheme are shown in Fig. 13.

6.0 QUANTUM LATTICE METHODS AND LBM FOR QUANTUM HYDRODYNAMICS

6.1 Type I: Lattice methods for quantum systems using classical computers

6.1.1 Very (very) brief reminder about equations of Quantum Physics

Lattice-based numerical methods discussed in this chapter are essentially designed to solve some basic equations of Quantum Physics. Therefore, before introducing the numerical approaches, we remind here the continuous equations that will be useful hereafter.

The Dirac equation for a free particle of mass m in 3D is

$$\frac{\partial \boldsymbol{\psi}}{\partial t} + c\left(-\boldsymbol{\alpha}^x \frac{\partial}{\partial x} + \beta \frac{\partial}{\partial y} - \boldsymbol{\alpha}^z \frac{\partial}{\partial z}\right)\boldsymbol{\psi} = -\mathrm{i}\frac{mc^2}{\hbar}\boldsymbol{\alpha}^y \boldsymbol{\psi} = -\mathrm{i}\omega_c \boldsymbol{\alpha}^y \boldsymbol{\psi} \tag{106}$$

where $\boldsymbol{\psi}$ and ω_c are the Dirac quadrispinor and the Compton frequency, respectively. The standard 4×4

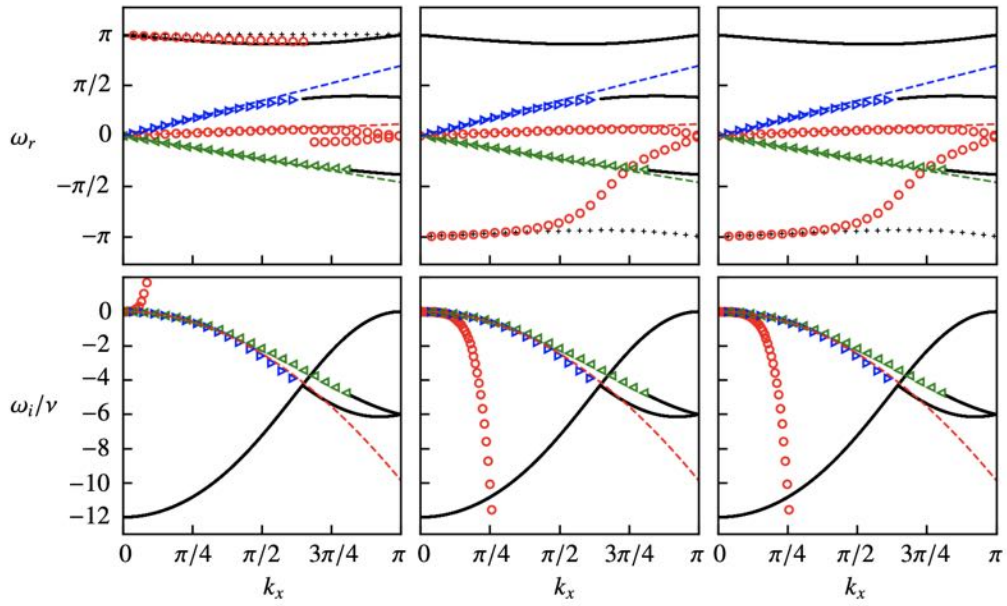

Figure 12: Linearized Stability Analysis of some regularized versions of the SRT-BGK scheme on the D2Q9 lattice (left: Projective Regularization, middle: Recursive Regularization - first version, right: Recursive Regularization - second version). Same caption as preceding figure. From [200].

Dirac matrices are defined as

$$\boldsymbol{\alpha}^x = \begin{pmatrix} 0 & 0 & 0 & 1 \\ 0 & 0 & 1 & 0 \\ 0 & 1 & 0 & 0 \\ 1 & 0 & 0 & 0 \end{pmatrix}, \boldsymbol{\alpha}^y = \begin{pmatrix} 0 & 0 & 0 & -\mathrm{i} \\ 0 & 0 & \mathrm{i} & 0 \\ 0 & -\mathrm{i} & 0 & 0 \\ \mathrm{i} & 0 & 0 & 0 \end{pmatrix}, \tag{107a}$$

$$\boldsymbol{\alpha}^z = \begin{pmatrix} 0 & 0 & 1 & 0 \\ 0 & 0 & 0 & -1 \\ 1 & 0 & 0 & 0 \\ 0 & -1 & 0 & 0 \end{pmatrix}, \boldsymbol{\beta} = \begin{pmatrix} 1 & 0 & 0 & 0 \\ 0 & 0 & 1 & 0 \\ 0 & 0 & -1 & 0 \\ 0 & 0 & 0 & -1 \end{pmatrix}, \tag{107b}$$

It is known that the Schrödinger equation can be derived from the Dirac equation in the non-relativistic limit by summation upon the four components of the quadrispinor, i.e. the complex wave function Ψ appearing the the Schrödinger equation is defined as $\Psi = \sum_{i=1,4} \psi_i$.

A classical formulation of the Schrödinger equation is

$$\mathbf{i}\hbar\frac{\partial\Psi}{\partial t} = -\frac{\hbar^2}{2m}\nabla^2\Psi + V\Psi \tag{108}$$

where V is a potential. Using the Magdelung formulation

$$\Psi(\mathbf{x},t) = \sqrt{\rho(\mathbf{x},t)}e^{\mathbf{i}\theta(\mathbf{x},t)/2}, \quad \rho = |\Psi|^2, \quad \mathbf{v} = \nabla\theta \tag{109}$$

and an *ad hoc* rescaling, one obtains the equivalent set of two equations with hydrodynamic-like features:

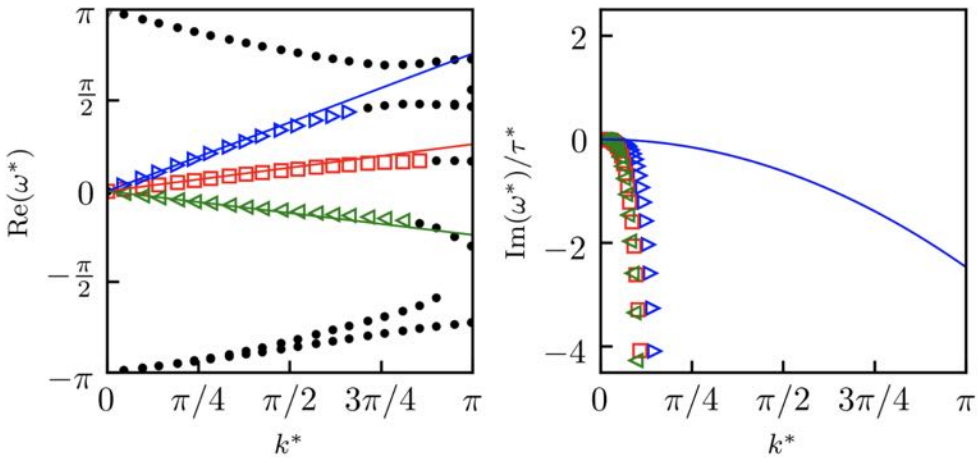

Figure 13: Linearized Stability Analysis of the Hybrid Recursive Regularized scheme on the D2Q9 lattice. Left: phase speed of the 9 numerical modes. Right: numerical viscosity normalized by the physical viscosity. Symbols denote observable physical modes at a given normalized wavenumber $k\Delta x$; Green triangles: upstream travelling acoustic mode, Blue triangles: downstream travelling acoustic mode, Red squares: vorticity mode. From [201].

$$\frac{\partial \rho}{\partial t} + \nabla \cdot (\rho \mathbf{v}) = 0 \tag{110a}$$

$$\rho \left(\frac{\partial \mathbf{v}}{\partial t} + \mathbf{v} \cdot \nabla \mathbf{v} \right) = -g \nabla (\rho^2) + 2\rho \nabla \left(\frac{\nabla^2 \sqrt{\rho}}{\sqrt{\rho}} \right) \tag{110b}$$

which are referred to as the Gross-Pitaevskii equations, that are commonly used for the analysis of Quantum Turbulence dynamics (see [203–208] for reviews about Quantum Turbulence).

The Dirac equation can also be rewritten as the following fluid-like equation

$$\frac{\partial (\boldsymbol{\psi}^\dagger \boldsymbol{\psi})}{\partial t} + c \nabla (\boldsymbol{\psi}^\dagger \boldsymbol{\alpha} \boldsymbol{\psi}) = 0 \tag{111}$$

which emphasizes the formal analogy with fluid mechanics equations.

6.1.2 Quantum LBM for the Dirac and Schrödinger equations

The Quantum Lattice-Boltzmann Method (QLBM) proposed coined by Succi and Benzi in 1993 [209–214] aims at solving the Dirac equation to obtain solutions of the non-relativistic Schrödinger equation. The rationale to develop QLBM is the formal analogy that exists between the derivation of this equation from the relativistic Dirac equation and the derivation of Navier-Stokes equations from the Boltzmann equation. Here, the proposed method is used to solve a non-hydrodynamic equations, not using it as a fully general numerical method as in classical LBM, but on the ground of a formal analogy.

In the QLBM approach, the distribution functions f_i of LBM will be assimilated to the wave functions composing the quadrispinor $\boldsymbol{\psi} = (\psi_1, \psi_2, \psi_3, \psi_4)^T$) (i.e. its four components) in the Dirac equation. The discrete velocity in LBM will be associated to the streaming matrice $\mathbf{L} = c(-\boldsymbol{\alpha}^x, \boldsymbol{\beta}, -\boldsymbol{\alpha}^z)$. The collision operator will be the analogue of the scattering term that appears in the r.h.s of (106).

The development of an LBM-type numerical method for the Dirac equation is not a straightforward extension since the operator $\mathbf{L}$ cannot be diagonalized in all directions at the same time. Therefore a directional splitting method must be used to recast the full problem as a sequence of three 1D problems, an additional rotation step being required between each monodimensional sequence.

The sketch of QLBM in 3D is

- **Step 1**: time integration along direction z
  - **Compute Collision**

$$\boldsymbol{\psi}_z^{coll,z}(\mathbf{x}) = \widehat{Q}\boldsymbol{\psi}(\mathbf{x},t)$$

    where $\widehat{Q}$ denotes the collision matrix (see below)
  - **Compute Streaming**

$$\boldsymbol{\psi}_z(\mathbf{x}+\mathbf{c}_z\Delta z) = S_z\boldsymbol{\psi}^{coll,z}(\mathbf{x})$$

    where $\mathbf{c}_z$ and S_z are the velocity vector in direction z and the streaming operator in that direction, respectively.
- **Step 2**: time integration along direction y
  - **Compute Rotation**

$$\boldsymbol{\psi}(\mathbf{x})_{yz} = Y\boldsymbol{\psi}_z(\mathbf{x}), \quad \widehat{Q}^y = Y^{-1}\widehat{Q}Y$$

    where Y is the rotation matrix from direction z to direction y
  - **Compute Collision**

$$\boldsymbol{\psi}^{coll,y}(\mathbf{x}+\mathbf{c}_z\Delta z) = \widehat{Q}^y\boldsymbol{\psi}_{yz}(\mathbf{x}+\mathbf{c}_z\Delta z)$$

  - **Compute Streaming**

$$\boldsymbol{\psi}_{yz}(\mathbf{x}+\mathbf{c}_y\Delta y+\mathbf{c}_z\Delta z) = \boldsymbol{\psi}^{coll,y}(\mathbf{x}+\mathbf{c}_z\Delta z)$$

    where $\mathbf{c}_y$ and S_y are the velocity vector in direction z and the streaming operator in that direction, respectively.
- **Step 3**: time integration along direction x
  - **Compute Rotation**

$$\boldsymbol{\psi}_{xyz}(\mathbf{x}) = X\boldsymbol{\psi}_{yz}(\mathbf{x}), \quad \widehat{Q}^x = X^{-1}\widehat{Q}^yX$$

    where X is the rotation matrix from direction y to direction x
  - **Compute Collision**

$$\boldsymbol{\psi}^{coll,x}(\mathbf{x}+\mathbf{c}_y\Delta y+\mathbf{c}_z\Delta z) = \widehat{Q}^x\boldsymbol{\psi}_{xyz}(\mathbf{x}+\mathbf{c}_y\Delta y+\mathbf{c}_z\Delta z)$$

– **Compute Streaming**

$$\boldsymbol{\psi}_{xyz}(\mathbf{x}+\mathbf{c}_x\Delta x+\mathbf{c}_y\Delta z+\mathbf{c}_z\Delta z)=\boldsymbol{\psi}^{coll,x}(\mathbf{x}+\mathbf{c}_y\Delta y+\mathbf{c}_z\Delta z)$$

where $\mathbf{c}_x$ and S_x are the velocity vector in direction z and the streaming operator in that direction, respectively.

- **Step 4**: Final update

$$\boldsymbol{\psi}(\mathbf{x}+\mathbf{c}_x\Delta x+\mathbf{c}_y\Delta z+\mathbf{c}_z\Delta z,t+\Delta t)=Y^{-1}X^{-1}\boldsymbol{\psi}_{xyz}(\mathbf{x}+\mathbf{c}_x\Delta x+\mathbf{c}_y\Delta z+\mathbf{c}_z\Delta z)$$

It is important noting that the collision matrix $\widehat{Q}$ is not the collision matrix associated to the 1D Dirac equation. Its expression is dimension-dependent. The reader is referred to [215] for its expression in 2D. This algorithm doesn't belong to the class of Lattice-Boltzmann Method *stricto sensu*. As a matter of fact, it is a regular numerical method to solve the Dirac equation, based on both a directional splitting and a first order operator splitting in each direction. The operator splitting is such that it shares some features of LBM, including the fact that there exists a hierarchy of continuous equations.

As a conclusion, QLBM is a classical numerical method to solve the Dirac equation that looks like a LBM-type algorithm for the Schrödinger equation, in the same way as LBM is a numerical method for the Discrete Velocity Boltzmann Equation that provides solutions of the macroscopic hydrodynamic equation.

QLBM has been used to compute some elementary test cases, e.g. free particule propagation, harmonic oscillator and scattering barrier.

6.1.3 Unitary Qbit Lattice Gas Algorithm for the Gross-Pitaevskii equation

Another method to solve the scalar Gross-Pitaevskii equations (110) and other variants of the Schrödinger equation was developed by Yepez, Vahala, Vahala and colleagues since the 1990s in a series of papers [216–229], which is referred to as the Unitary Qbit Lattice Gas Algorithm (UQLGA).

In this approach, two Qbits are defined at each lattice point to follow the time evolution of the scalar wave function Ψ appearing in the Schrödinger equation (108), leading to the definition of 2^2 states. The later are encoded on a classical computer using the two complex amplitudes $\alpha(\mathbf{x},t)$ and $\beta(\mathbf{x},t)$. Numerically, the two-spinor vector $\psi(\mathbf{x},t)$ is updated at each time step at each lattice point, with

$$\psi(\mathbf{x},t)=\begin{pmatrix}\alpha(\mathbf{x},t)\\ \beta(\mathbf{x},t)\end{pmatrix},\quad \alpha\in\mathbb{C},\beta\in\mathbb{C} \tag{112}$$

The algorithm is splitted into three substeps at each time step, which are symmetrized in order to recover a higher-order method, in agreement Strang's analysis of spliting methods:

- **Compute unitary collision** to locally entangle α and β. This is performed using the "square-root-of-swap" operator as a collision operator, which is associated to the 2×2 matrix:

$$C=\frac{1}{2}\begin{pmatrix}1-\mathrm{i} & 1+\mathrm{i}\\ 1+\mathrm{i} & 1-\mathrm{i}\end{pmatrix},\quad C^2=\begin{pmatrix}\alpha\\ \beta\end{pmatrix}=\begin{pmatrix}\beta\\ \alpha\end{pmatrix},\quad C^4=Id \tag{113}$$

- **Compute unitary streaming** to shift the post-collision amplitudes to the neighboring points of the lattice. To this end, the following general streaming operator is introduced:

$$S_{\Delta x,1}\begin{pmatrix}\alpha(\mathbf{x},t)\\ \beta(\mathbf{x},t)\end{pmatrix}=\begin{pmatrix}\alpha(\mathbf{x}+\Delta\mathbf{x},t)\\ \beta(\mathbf{x},t)\end{pmatrix},\quad S_{-\Delta x,2}\begin{pmatrix}\alpha(\mathbf{x},t)\\ \beta(\mathbf{x},t)\end{pmatrix}=\begin{pmatrix}\alpha(\mathbf{x},t)\\ \beta(\mathbf{x}-\Delta\mathbf{x},t)\end{pmatrix} \tag{114}$$

  where the subscripts 1 and 2 denote shifts applied to α and β, respectively.

- **Compute exponential phase operator effect** to account for nonlinear terms of the Gross-Pitaevskii equations. This operator is defined as $\exp(-\mathrm{i}\epsilon^2\Omega)$, where $\epsilon \ll 1$ is a small parameter.

A time step in practice computed as follows:

$$\psi(\mathbf{x},t+\Delta t)=U_2(\Omega/2)U_1(\Omega/2)\psi(\mathbf{x},t) \tag{115}$$

where $U_\gamma(\Omega)$ is the following evolution operator:

$$U_\gamma(\Omega)=J^2_{x\gamma}J^2_{y\gamma}J^2_{z\gamma}e^{-\mathrm{i}\epsilon^2\Omega},\quad J_{x\gamma}=S_{-\Delta x,\gamma}CS_{\Delta x,\gamma}C \tag{116}$$

Using the diffusive scaling $\Delta t = O(\epsilon^2)$ and $\Delta x = 0(\epsilon)$, Taylor series expansion leads to the following Equivalent Differential Equation

$$\mathrm{i}\frac{\partial\psi}{\partial t}=-\left(-\frac{1}{2}\sigma_x\nabla^2+\Omega\right)+O(\epsilon^2),\quad \sigma_x=\begin{pmatrix}0&1\\1&0\end{pmatrix} \tag{117}$$

The scalar Gross-Pitaevskii equation solution ϕ is recovered by adding α and β, $\phi=\alpha+\beta$, rescaling the gradient by a factor $1/a$ and chosing $\Omega = g|\phi|^2-1$, leading to

$$\mathrm{i}\frac{\partial\phi}{\partial t}=-\nabla^2\phi+a(g|\phi|^2-1)\phi+O(\epsilon^2) \tag{118}$$

This algorithm is unconditionally stable since it is defined by a unitary operation at each time step. This property is shared by classical Boolean Lattice Gas Automata. It has been proved to very efficient on classical massively parallel computers (up to 163 000 core on a Blue Gene computer), and then allowed for large-scale simulations of quantum turbulence on 5760^3 computational grids using 12 000 cores. One of the most striking use of this method in the field of hydrodynamics is a landmark simulation of superfluid turbulence [222] that exhibits two inertial ranges : the classical Kolmogorov range with a $k^{-5/3}$ scaling at large hydrodynamic scales and a second inertial range at sub-hydrodynamic range, associated to Kelvin waves and quantized vortices dynamics, with a k^{-3} scaling (see Fig. 14).

6.1.4 LBM for the Gross-Pitaevskii equation

A "true classical" Lattice-Boltzmann Method that solves the following (rescaled) scalar Gross-Pitaevskii equations has been proposed by Wang [230]:

$$\mathrm{i}\frac{\partial\phi}{\partial t}=-\frac{1}{2}\nabla^2\phi+|\phi|^2\phi-V\phi+O(\epsilon^2) \tag{119}$$

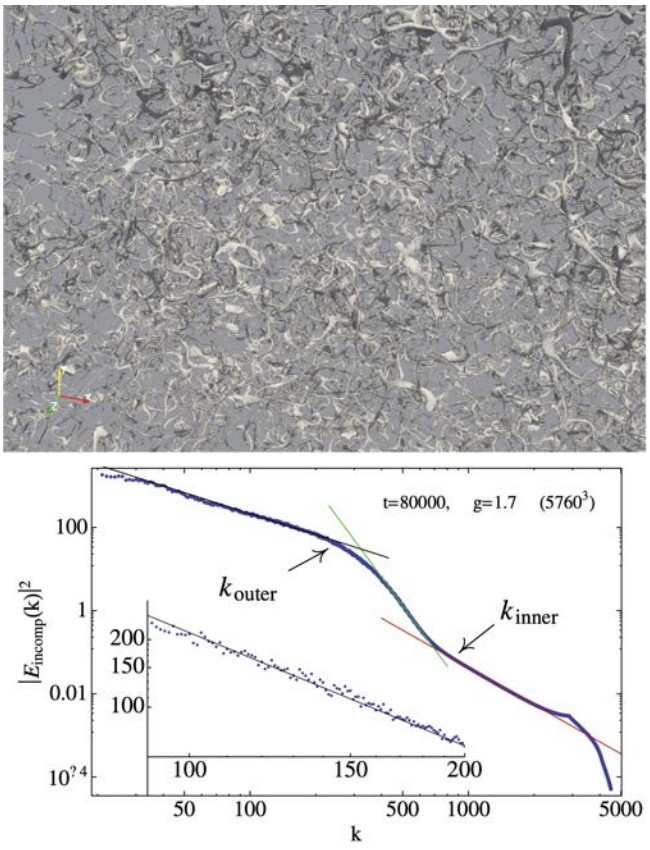

Figure 14: UQLGA simulation of superfluid turbulence on a 5760^3 grid. Top: instantaneous view of the vortical field showing the existence of quantum vortices. Bottom: kinetic energy spectrum of the solenoidal part of the velocity field showing the existence of two inertial ranges. From [222].

This Lattice Boltzmann Method is defined by the following relations on a D2Q9 lattice:

$$\sum_{i=0,8} f_i = \sum_{i=0,8} f_i^{eq} = \mathrm{i}\phi, \quad f_i^{eq} = \begin{cases} \left(\mathrm{i} - \frac{3}{\tau 2 c_s^2}\right)\phi & i = 0 \\ \frac{\phi}{4\tau c_s^2} & \alpha = 1,2,3,4 \\ \frac{\phi}{8\tau c_s^2} & \alpha = 5,6,7,8 \end{cases} \tag{120}$$

where τ is the relaxation time of the SRT-BGK collision operator. A forcing term F_i is added for the sake of consistency with

$$F_i = \frac{-V\phi + |\phi|^2\phi}{9\tau}, \forall i \tag{121}$$

This method has been assessed on 1D and 2D elementary test cases.

6.1.5 LBM for the Hall-Vinen-Bekarevich-Khalatnikov equations

The last example presented here is a classical Lattice Boltzmann Method to analyze superfluid hydrodynamics and turbulence solving the governing equations of the Hall-Vinen-Bekarevich-Khalatnikov (HVBK) model,

e.g. [231, 232]. The HVBK model originates in the modelling of superfluid hydrodynamics by Titza and Landau as the results of the coupling of an incompressible inviscid fluid with a viscous incompressible fluid, the coupling origination in a so-called mutual friction mechanism. Introducing a normal fluid component with velocity $\mathbf{u}_n$, viscosity $\mu_n$and density ρ_n and an inviscid superfluid component with velocity $\mathbf{u}_s$ and density ρ_s, the momentum equations reads

$$\rho_s \left(\frac{\partial \mathbf{u}_s}{\partial t} + \mathbf{u}_s \nabla \mathbf{u}_s \right) = -\frac{\rho_s}{\rho} \nabla p + \rho_s s \nabla T + \frac{\rho_s \rho_n}{2\rho} \nabla (\mathbf{u}_n - \mathbf{u}_s)^2 - \mathbf{f}_{ns} \tag{122}$$

$$\rho_n \left(\frac{\partial \mathbf{u}_n}{\partial t} + \mathbf{u}_n \nabla \mathbf{u}_n \right) = -\frac{\rho_n}{\rho} \nabla p - \rho_s s \nabla T - \frac{\rho_s \rho_n}{2\rho} \nabla (\mathbf{u}_n - \mathbf{u}_s)^2 + \mathbf{u}_{ns} + \mu_n \nabla^2 \mathbf{u}_n \tag{123}$$

where μ_n is the normal fluid viscosity, along with

$$\nabla \cdot \mathbf{u}_s = 0, \quad \nabla \cdot \mathbf{u}_n = 0 \tag{124}$$

where $\mathbf{f}_{ns}$ denotes the mutual friction force, with

$$\mathbf{f}_{ns} = -\frac{\rho_n \rho_s}{2\rho} \left(B \hat{\boldsymbol{\omega}} \times [\boldsymbol{\omega} \times (\mathbf{u}_s - \mathbf{u}_n)] + B' \hat{\boldsymbol{\omega}} \times (\mathbf{u}_s - \mathbf{u}_n) \right) \tag{125}$$

where $\boldsymbol{\omega} = \text{curl}\,(\mathbf{u}_n)$ denotes the vorticity and $\hat{\boldsymbol{\omega}} = \boldsymbol{\omega}/\|\boldsymbol{\omega}\|$ is the associated unit vector, and B and B' are tabulated coefficients.

In [231, 232], classical SRT-BGK for athermal flows on D2Q9 and D3Q19 grid were used, with a forcing term to account for the mutual friction. Since the basic HVBK model is a macroscopic hydrodynamic model, there is no specific modification of the classical LBM approach to solve it. A major achievement was performed by Inui and Tsubota [231] who have simulated 3D quantum vortices dynamics, as illustrated in Fig. 15.

6.2 Type III: Lattice methods for classical systems using quantum computers

We now discuss (briefly) some features of the implementation of Lattice-type methods for classical CFD problems on Quantum Computers, i.e. using quantum circuits/gates and quantum algorithm. Before that, let us remind that the four steps of the development of a method for practical engineering purposes:

- **Step 1: Consistency**: the method should provide solutions that are physically consistent, in the sens that main physical mechanisms are captured
- **Step 2: Robustness**: the method must be robust enough to allow for the simulation of a broad range of configurations without need for ad hoc tuning for each new computational setup
- **Step 3: Accuracy**: the results must be accurate enough to be reliable, and there should exist ways to increase the accuracy if needed without modifying the numerical method, e.g. refinement
- **Step 4: Speed/computational cost**: the method should be fast enough to be compatible with the engineering cycle (typically a few hours/ tens of hours to compute an industrial flow).

Some remarks may be done about the development of industrial CFD tools on Quantum Computers, i.e. using quantum circuits. Since their architectures and underlying physics are very different from those of classical computers, one must face the following problems:

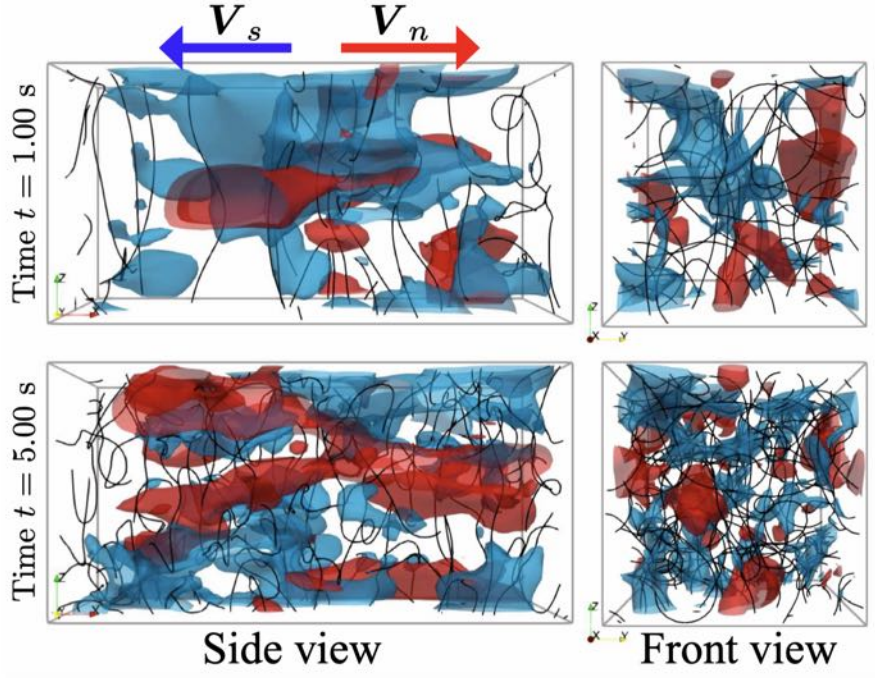

Figure 15: LBM simulation of the development of a quantum vortex tangle in superfluid turbulence with D3Q19 lattice solving the HVBK hydrodynamic model. Black lines: quantum vortices. Blue and red isosurfaces: isovalues of the instantaneous normal velocity field. From [231].

- Most existing methods can't be straightforwardly reimplemented, since some key parts of the classical algorithm are not compatible with quantum circuit "as is". To alleviate this problem, classical numerical methods/algorithms must be rewritten in order to use existing quantum algorithms (if possible), or must be modified to do that. In the worse case, a fully new method must be developed. In the case of LBM, the problem is the nonlinearity of the collision model.
- The method must not be sensitive to noise, since existing machine still produce noisy results compared with classical computers on which the sensitivity of the computed solution to round-off errors is identified to be also an issue.
- Speed-up of the simulation: the numerical method should be based on quantum algorithms that exhibit a significant speed-up (polynomial, exponential) with their classical counterparts.
- The pre-processing step and the measure step must be efficiently implemented.

Looking at existing implementations of Lattice-type method for CFD (see also other lectures in this series), one can observed that collision operators (more precisely their nonlinear character) are the main problem. A collisionless LBM was considered by Todorova and Steijl [233] in which this issue was bypassed, but at the cost of a reduced physical consistency (as a matter of fact, collisionless can only mimic inviscid fluid dynamics). Another approach was followed by Budinski [152], who used the Streamfunction-Vorticity formulation of the Navier–Stokes equations in 2D for incompressible fluids (see Section 4.2). Doing that, the problem simplifies as the coupling of a Poisson equation and an advection-diffusion equation discretized using a linear collision

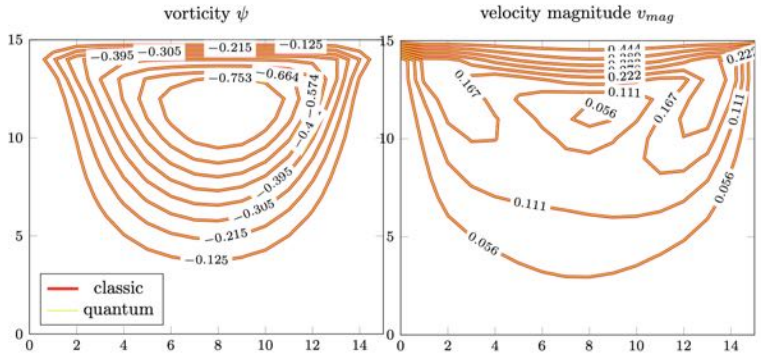

Figure 16: Comparison of the results obtained on a classical computer and with quantum algorithms in the case of a 2D steady laminar cavity flow. Navier–Stokes equations are solved in the $\psi - \omega$ formulation using LBM on a D2Q5 lattice. From [152], with courtesy of L. Budinski @ Quanscient.

model, yielding very satisfactory results compared to the same LBM implemented on a classical computer (see Fig. 16). The same author had previously implemented the linear advection-diffusion case [234]. Therefore, the nonlinearity issue must be solved to obtain fully efficient LBM on quantum computers.

In an earlier work dealing with LGA, Chen et al. [235] did implement the Yepez' LGA method on a hybrid system to solve the 1D nonlinear Burger equation. Here, Quantum-Information Processors were modelled using Nuclear Magnetic Resonance.The main identified problems were the robustness and the accuracy, both arising in the collision step. A randomization step was added to prevent the error pile-up. Theoretical problems dealing with the implementation of the collision step in Lattice Gas Automata have been pointed out recently by Love [236].

ACKNOWLEDGMENTS

Fruitful and enlightning discussions during the last years with young outstanding researchers are warmly acknowledged. For the present content, I'm specifically indebted to Thomas Astoul, Pierre Boivin, Thomas Coratger, Gabriel Farag, Yongliang Feng, Shaolong Guo, Jérôme Jacob, Florian Renard, Gauthier Wissocq and Song Zhao.

REFERENCES

[1] Timm, K., Kusumaatmaja, H., Kuzmin, A., Shardt, O., Silva, G., and Viggen, E., *The lattice Boltzmann method: principles and practice*, Springer, 2016.

[2] Succi, S., *The lattice Boltzmann equation: for fluid dynamics and beyond*, Oxford university press, 2001.

[3] Nourgaliev, R. R., Dinh, T.-N., Theofanous, T. G., and Joseph, D., "The lattice Boltzmann equation method: theoretical interpretation, numerics and implications," *International Journal of Multiphase Flow*, Vol. 29, No. 1, 2003, pp. 117–169.

[4] Chen, S. and Doolen, G. D., "Lattice Boltzmann method for fluid flows," *Annual review of fluid mechanics*, Vol. 30, No. 1, 1998, pp. 329–364.

[5] Gradner, M., "The Fantastic Combinations of John Conway's New Solitaire Game Life [J]," *Scientific American*, Vol. 223, No. 4, 1970, pp. 120–123.

[6] Benioff, P., "The computer as a physical system: A microscopic quantum mechanical Hamiltonian model of computers as represented by Turing machines," *Journal of statistical physics*, Vol. 22, No. 5, 1980, pp. 563–591.

[7] Bennett, C. H., "The thermodynamics of computation: A review," *International Journal of Theoretical Physics*, Vol. 21, No. 12, 1982, pp. 905–940.

[8] Wolfram, S., "Universality and complexity in cellular automata," *Physica D: Nonlinear Phenomena*, Vol. 10, No. 1-2, 1984, pp. 1–35.

[9] Durand, B. and Róka, Z., "The game of life: universality revisited," *Cellular automata*, Springer, 1999, pp. 51–74.

[10] Rennard, J.-P., "Implementation of logical functions in the Game of Life," *Collision-based computing*, Springer, 2002, pp. 491–512.

[11] Chopard, B. and Droz, M., *Cellular automata modeling of physical systems*, Cambridge University Press, 1998.

[12] Rothman, D. and Zaleski, S., *Lattice-Gas Cellular Automata*, Cambridge University Press, 1997.

[13] Wolf-Gladrow, D., *Lattice Gas Cellular Automata and Lattice Boltzmann Models*, Springer, 2000.

[14] Hardy, J., Pomeau, Y., and De Pazzis, O., "Time evolution of a two-dimensional model system. I. Invariant states and time correlation functions," *Journal of Mathematical Physics*, Vol. 14, No. 12, 1973, pp. 1746–1759.

[15] Frisch, U., Hasslacher, B., and Pomeau, Y., "Lattice-gas automata for the Navier-Stokes equation," *Physical review letters*, Vol. 56, No. 14, 1986, pp. 1505.

[16] Hasslacher, B., Frisch, U., d Humieres, D., Rivet, J., Lallemand, P., and Pomeau, Y., "Lattice gas hydrodynamics in two and three dimensions," *Complex systems*, Vol. 1, No. 4, 1987, pp. 649–708.

[17] Chen, H., Chen, S., and Matthaeus, W. H., "Recovery of the Navier-Stokes equations using a lattice-gas Boltzmann method," *Physical review A*, Vol. 45, No. 8, 1992, pp. R5339.

[18] Parsa, M. R., *Lattice gases with molecular dynamics collision operator*, Ph.D. thesis, North Dakota State University, 2018.

[19] Rivet, J. and Boon, J., *Lattice Gas Hydrodynamics*, Cambridge University Press, 2001.

[20] Boghosian, B. M., Yepez, J., Alexander, F. J., and Margolus, N. H., "Integer lattice gases," *Physical Review E*, Vol. 55, No. 4, 1997, pp. 4137.

[21] Blommel, T. and Wagner, A. J., "Integer lattice gas with Monte Carlo collision operator recovers the lattice Boltzmann method with Poisson-distributed fluctuations," *Physical Review E*, Vol. 97, No. 2, 2018, pp. 023310.

[22] Parsa, M. R. and Wagner, A. J., "Lattice gas with molecular dynamics collision operator," *Physical Review E*, Vol. 96, No. 1, 2017, pp. 013314.

[23] Parsa, M. R., Pachalieva, A., and Wagner, A. J., "Validity of the molecular-dynamics-lattice-gas global equilibrium distribution function," *International Journal of Modern Physics C*, Vol. 30, No. 10, 2019, pp. 1941007.

[24] Parsa, M. R. and Wagner, A. J., "Large fluctuations in nonideal coarse-grained systems," *Physical Review Letters*, Vol. 124, No. 23, 2020, pp. 234501.

[25] Pachalieva, A. and Wagner, A. J., "Connecting lattice Boltzmann methods to physical reality by coarse-graining Molecular Dynamics simulations," *arXiv preprint arXiv:2109.05009*, 2021.

[26] Parsa, M. R., Kim, C., and Wagner, A. J., "Nonuniqueness of fluctuating momentum in coarse-grained systems," *Physical Review E*, Vol. 104, No. 1, 2021, pp. 015304.

[27] Pachalieva, A. and Wagner, A. J., "Molecular dynamics lattice gas equilibrium distribution function for Lennard–Jones particles," *Philosophical Transactions of the Royal Society A*, Vol. 379, No. 2208, 2021, pp. 20200404.

[28] Seekins, N. and Wagner, A. J., "Integer lattice gas with a sampling collision operator for the fluctuating diffusion equation," *Physical Review E*, Vol. 105, No. 3, 2022, pp. 035303.

[29] Doolen, G., Frisch, U., Hasslacher, B., Orszag, S., and Wolfram, W., *Lattice-Gas Methods for Partial Differential Equations*, Taylor & Francis, 1990.

[30] McNamara, G. R. and Zanetti, G., "Use of the Boltzmann equation to simulate lattice-gas automata," *Physical review letters*, Vol. 61, No. 20, 1988, pp. 2332.

[31] Qian, Y.-H., d'Humières, D., and Lallemand, P., "Lattice BGK models for Navier-Stokes equation," *EPL (Europhysics Letters)*, Vol. 17, No. 6, 1992, pp. 479.

[32] Higuera, F. J. and Jiménez, J., "Boltzmann approach to lattice gas simulations," *EPL (Europhysics Letters)*, Vol. 9, No. 7, 1989, pp. 663.

[33] Higuera, F., Succi, S., and Benzi, R., "Lattice gas dynamics with enhanced collisions," *EPL (Europhysics Letters)*, Vol. 9, No. 4, 1989, pp. 345.

[34] He, X. and Luo, L.-S., "Theory of the lattice Boltzmann method: From the Boltzmann equation to the lattice Boltzmann equation," *Physical review E*, Vol. 56, No. 6, 1997, pp. 6811.

[35] Abe, T., "Derivation of the lattice Boltzmann method by means of the discrete ordinate method for the Boltzmann equation," *Journal of Computational Physics*, Vol. 131, No. 1, 1997.

[36] Shan, X., Yuan, X.-F., and Chen, H., "Kinetic theory representation of hydrodynamics: a way beyond the Navier–Stokes equation," *Journal of Fluid Mechanics*, Vol. 550, 2006, pp. 413–441.

[37] Jin, S., "Asymptotic preserving (AP) schemes for multiscale kinetic and hyperbolic equations: a review," *Lecture notes for summer school on methods and models of kinetic theory (M&MKT), Porto Ercole (Grosseto, Italy)*, 2010, pp. 177–216.

[38] Hirsch, C., "Numerical computation of internal and external flows. Vol. 1-Fundamentals of numerical disretization," *Wiley*, 1989.

[39] Sengupta, T. K., Dipankar, A., and Sagaut, P., "Error dynamics: beyond von Neumann analysis," *Journal of Computational Physics*, Vol. 226, No. 2, 2007, pp. 1211–1218.

[40] Christiansen, S. H., Munthe-Kaas, H. Z., and Owren, B., "Topics in structure-preserving discretization," *Acta Numerica*, Vol. 20, 2011, pp. 1–119.

[41] Lallemand, P. and Luo, L.-S., "Hybrid finite-difference thermal lattice Boltzmann equation," *International Journal of Modern Physics B*, Vol. 17, No. 01n02, 2003, pp. 41–47.

[42] Farag, G., Zhao, S., Coratger, T., Boivin, P., Chiavassa, G., and Sagaut, P., "A pressure-based regularized lattice-Boltzmann method for the simulation of compressible flows," *Physics of Fluids*, Vol. 32, No. 6, 2020, pp. 066106.

[43] Wissocq, G., Coratger, T., Farag, G., Zhao, S., Boivin, P., and Sagaut, P., "Restoring the conservativity of characteristic-based segregated models: application to the hybrid lattice Boltzmann method," *Physics of Fluids*, Vol. 34, No. 4, 2022, pp. 046102.

[44] Farag, G., Coratger, T., Wissocq, G., Zhao, S., Boivin, P., and Sagaut, P., "A unified hybrid lattice-Boltzmann method for compressible flows: Bridging between pressure-based and density-based methods," *Physics of Fluids*, Vol. 33, No. 8, 2021, pp. 086101.

[45] Renard, F., Feng, Y., Boussuge, J.-F., and Sagaut, P., "Improved compressible hybrid lattice Boltzmann method on standard lattice for subsonic and supersonic flows," *Computers and Fluids*, Vol. 219, 2021, pp. 104867.

[46] Feng, Y., Boivin, P., Jacob, J., and Sagaut, P., "Hybrid recursive regularized thermal lattice Boltzmann model for high subsonic compressible flows," *Journal of Computational Physics*, Vol. 394, 2019, pp. 82–99.

[47] Junk, M. and Klar, A., "Discretizations for the incompressible Navier–Stokes Equations based on the lattice Boltzmann method," *SIAM Journal on Scientific Computing*, Vol. 22, No. 1, 2000, pp. 1–19.

[48] Asinari, P., Ohwada, T., Chiavazzo, E., and Di Rienzo, A. F., "Link-wise artificial compressibility method," *Journal of Computational Physics*, Vol. 231, No. 15, 2012, pp. 5109–5143.

[49] Dubois, F., Lallemand, P., Obrecht, C., and Tekitek, M. M., "Lattice Boltzmann model approximated with finite difference expressions," *Computers & Fluids*, Vol. 155, 2017, pp. 3–8.

[50] Feng, Y., Guo, S., Jacob, J., and Sagaut, P., "Solid wall and open boundary conditions in hybrid recursive regularized lattice Boltzmann method for compressible flows," *Physics of Fluids*, Vol. 31, No. 12, 2019, pp. 126103.

[51] Degrigny, J., Cai, S.-G., Boussuge, J.-F., and Sagaut, P., "Improved wall model treatment for aerodynamic flows in LBM," *Computers & Fluids*, Vol. 227, 2021, pp. 105041.

[52] Cai, S.-G., Degrigny, J., Boussuge, J.-F., and Sagaut, P., "Coupling of turbulence wall models and immersed boundaries on Cartesian grids," *Journal of Computational Physics*, Vol. 429, 2021, pp. 109995.

[53] Lagrava, D., Malaspinas, O., Latt, J., and Chopard, B., "Advances in multi-domain lattice Boltzmann grid refinement," *Journal of Computational Physics*, Vol. 231, No. 14, 2012, pp. 4808–4822.

[54] Feng, Y., Guo, S., Jacob, J., and Sagaut, P., "Grid refinement in the three-dimensional hybrid recursive regularized lattice Boltzmann method for compressible aerodynamics," *Physical Review E*, Vol. 101, No. 6, 2020, pp. 063302.

[55] Astoul, T., Wissocq, G., Boussuge, J.-F., Sengissen, A., and Sagaut, P., "Lattice Boltzmann method for computational aeroacoustics on non-uniform meshes: A direct grid coupling approach," *Journal of Computational Physics*, Vol. 447, 2021, pp. 110667.

[56] Astoul, T., Wissocq, G., Boussuge, J.-F., Sengissen, A., and Sagaut, P., "Analysis and reduction of spurious noise generated at grid refinement interfaces with the lattice Boltzmann method," *Journal of Computational Physics*, Vol. 418, 2020, pp. 109645.

[57] Cheylan, I., Favier, J., and Sagaut, P., "Immersed boundary conditions for moving objects in turbulent flows with the lattice-Boltzmann method," *Physics of Fluids*, Vol. 33, No. 9, 2021, pp. 095101.

[58] Yoo, H., Bahlali, M., Favier, J., and Sagaut, P., "A hybrid recursive regularized lattice Boltzmann model with overset grids for rotating geometries," *Physics of Fluids*, Vol. 33, No. 5, 2021, pp. 057113.

[59] Bahlali, M., Yoo, H., Favier, J., and Sagaut, P., "A lattice Boltzmann direct coupling overset approach for the moving boundary problem," *Physics of Fluids*, Vol. 33, No. 5, 2021, pp. 053607.

[60] Feng, Y., Miranda-Fuentes, J., Guo, S., Jacob, J., and Sagaut, P., "ProLB: A Lattice Boltzmann Solver of Large-Eddy Simulation for Atmospheric Boundary Layer Flows," *Journal of Advances in Modeling Earth Systems*, Vol. 13, No. 3, 2021, pp. e2020MS002107.

[61] Merlier, L., Jacob, J., and Sagaut, P., "Lattice-Boltzmann Large-Eddy Simulation of pollutant dispersion in street canyons including tree planting effects," *Atmospheric Environment*, Vol. 195, 2018, pp. 89–103.

[62] Merlier, L., Jacob, J., and Sagaut, P., "Lattice-Boltzmann large-eddy simulation of pollutant dispersion in complex urban environment with dense gas effect: Model evaluation and flow analysis," *Building and Environment*, Vol. 148, 2019, pp. 634–652.

[63] Jacob, J., Merlier, L., Marlow, F., and Sagaut, P., "Lattice Boltzmann Method-Based Simulations of Pollutant Dispersion and Urban Physics," *Atmosphere*, Vol. 12, No. 7, 2021, pp. 833.

[64] Jacob, J. and Sagaut, P., "Wind comfort assessment by means of large eddy simulation with lattice Boltzmann method in full scale city area," *Building and Environment*, Vol. 139, 2018, pp. 110–124.

[65] Marlow, F., Jacob, J., and Sagaut, P., "A multidisciplinary model coupling Lattice-Boltzmann-based CFD and a Social Force Model for the simulation of pollutant dispersion in evacuation situations," *Building and Environment*, Vol. 205, 2021, pp. 108212.

[66] Feng, Y., Sagaut, P., and Tao, W., "A three dimensional lattice model for thermal compressible flow on standard lattices," *Journal of Computational Physics*, Vol. 303, 2015, pp. 514–529.

[67] Feng, Y., Sagaut, P., and Tao, W.-Q., "A compressible lattice Boltzmann finite volume model for high subsonic and transonic flows on regular lattices," *Computers & Fluids*, Vol. 131, 2016, pp. 45–55.

[68] Guo, S., Feng, Y., Jacob, J., Renard, F., and Sagaut, P., "An efficient lattice Boltzmann method for compressible aerodynamics on D3Q19 lattice," *Journal of Computational Physics*, Vol. 418, 2020, pp. 109570.

[69] Frapolli, N., Chikatamarla, S., and Karlin, I., "Theory, analysis, and applications of the entropic lattice Boltzmann model for compressible flows," *Entropy*, Vol. 22, No. 3, 2020, pp. 370.

[70] Zhao, S., Farag, G., Boivin, P., and Sagaut, P., "Toward fully conservative hybrid lattice Boltzmann methods for compressible flows," *Physics of Fluids*, Vol. 32, No. 12, 2020, pp. 126118.

[71] Coratger, T., Farag, G., Zhao, S., Boivin, P., and Sagaut, P., "Large-eddy lattice-Boltzmann modeling of transonic flows," *Physics of Fluids*, Vol. 33, No. 11, 2021, pp. 115112.

[72] Wang, G., Zhao, S., Boivin, P., Serre, E., and Sagaut, P., "A new hybrid Lattice-Boltzmann method for thermal flow simulations in low-Mach number approximation," *Physics of Fluids*.

[73] Feng, Y., Tayyab, M., and Boivin, P., "A Lattice-Boltzmann model for low-Mach reactive flows," *Combustion and Flame*, Vol. 196, 2018, pp. 249–254.

[74] Hosseini, S. A., Safari, H., Darabiha, N., Thévenin, D., and Krafczyk, M., "Hybrid lattice Boltzmann-finite difference model for low Mach number combustion simulation," *Combustion and Flame*, Vol. 209, 2019, pp. 394–404.

[75] Tayyab, M., Zhao, S., Feng, Y., and Boivin, P., "Hybrid regularized lattice-Boltzmann modelling of premixed and non-premixed combustion processes," *Combustion and Flame*, Vol. 211, 2020, pp. 173–184.

[76] Boivin, P., Tayyab, M., and Zhao, S., "Benchmarking a lattice-Boltzmann solver for reactive flows: Is the method worth the effort for combustion?" *Physics of Fluids*, Vol. 33, No. 7, 2021, pp. 071703.

[77] Tayyab, M., Radisson, B., Almarcha, C., Denet, B., and Boivin, P., "Experimental and numerical lattice-Boltzmann investigation of the Darrieus–Landau instability," *Combustion and Flame*, Vol. 221, 2020, pp. 103–109.

[78] Hosseini, S., Abdelsamie, A., Darabiha, N., and Thévenin, D., "Low-Mach hybrid lattice Boltzmann-finite difference solver for combustion in complex flows," *Physics of Fluids*, Vol. 32, No. 7, 2020, pp. 077105.

[79] Bhairapurada, K., Denet, B., and Boivin, P., "A Lattice-Boltzmann study of premixed flames thermo-acoustic instabilities," *Combustion and Flame*, Vol. 240, 2022, pp. 112049.

[80] Sawant, N., Dorschner, B., and Karlin, I., "A lattice Boltzmann model for reactive mixtures," *Philosophical Transactions of the Royal Society A*, Vol. 379, No. 2208, 2021, pp. 20200402.

[81] Guo, S., Feng, Y., and Sagaut, P., "On the use of conservative formulation of energy equation in hybrid compressible lattice Boltzmann method," *Computers & Fluids*, Vol. 219, 2021, pp. 104866.

[82] Samanta, R., Chattopadhyay, H., and Guha, C., "A review on the application of lattice Boltzmann method for melting and solidification problems," *Computational Materials Science*, Vol. 206, 2022, pp. 111288.

[83] Krafczyk, M., Cerrolaza, M., Schulz, M., and Rank, E. ., "Analysis of 3D transient blood flow passing through an artificial aortic valve by Lattice–Boltzmann methods," *Journal of Biomechanics*, Vol. 31, No. 5, 1998, pp. 453–462.

[84] Papavassiliou, D., Pham, N., Kadri, O., and Voronov, R., "Lattice Boltzmann methods for bioengineering applications," *Numerical methods and advanced simulation in biomechanics and biological processes*, Elsevier, 2018, pp. 415–429.

[85] Chateau, S., D Ortona, U., Poncet, S., and Favier, J., "Transport and mixing induced by beating cilia in human airways," *Frontiers in physiology*, Vol. 9, 2018, pp. 161.

[86] Loiseau, E., Gsell, S., Nommick, A., Jomard, C., Gras, D., Chanez, P., D Ortona, U., Kodjabachian, L., Favier, J., and Viallat, A., "Active mucus–cilia hydrodynamic coupling drives self-organization of human bronchial epithelium," *Nature Physics*, Vol. 16, No. 11, 2020, pp. 1158–1164.

[87] Aidun, C. K. and Clausen, J. R., "Lattice-Boltzmann method for complex flows," *Annual review of fluid mechanics*, Vol. 42, 2010, pp. 439–472.

[88] Malaspinas, O., Fiétier, N., and Deville, M., "Lattice Boltzmann method for the simulation of viscoelastic fluid flows," *Journal of Non-Newtonian Fluid Mechanics*, Vol. 165, No. 23-24, 2010, pp. 1637–1653.

[89] Krafczyk, M., Tölke, J., Rank, E., and Schulz, M., "Two-dimensional simulation of fluid–structure interaction using lattice-Boltzmann methods," *Computers & Structures*, Vol. 79, No. 22-25, 2001, pp. 2031–2037.

[90] Owen, D., Leonardi, C., and Feng, Y., "An efficient framework for fluid–structure interaction using the lattice Boltzmann method and immersed moving boundaries," *International Journal for Numerical Methods in Engineering*, Vol. 87, No. 1-5, 2011, pp. 66–95.

[91] De Rosis, A., Falcucci, G., Ubertini, S., Ubertini, F., and Succi, S., "Lattice Boltzmann analysis of fluid-structure interaction with moving boundaries," *Communications in Computational Physics*, Vol. 13, No. 3, 2013, pp. 823–834.

[92] Geller, S., Tölke, J., and Krafczyk, M., "Lattice-Boltzmann method on quadtree-type grids for fluid-structure interaction," *Fluid-Structure Interaction*, Springer, 2006, pp. 270–293.

[93] Favier, J., Revell, A., and Pinelli, A., "A Lattice Boltzmann–Immersed Boundary method to simulate the fluid interaction with moving and slender flexible objects," *Journal of Computational Physics*, Vol. 261, 2014, pp. 145–161.

[94] Li, Z., Favier, J., D Ortona, U., and Poncet, S., "An immersed boundary-lattice Boltzmann method for single-and multi-component fluid flows," *Journal of Computational Physics*, Vol. 304, 2016, pp. 424–440.

[95] Li, Z. and Favier, J., "A non-staggered coupling of finite element and lattice Boltzmann methods via an immersed boundary scheme for fluid-structure interaction," *Computers & Fluids*, Vol. 143, 2017, pp. 90–102.

[96] O Brien, G. S., Nissen-Meyer, T., and Bean, C., "A lattice Boltzmann method for elastic wave propagation in a poisson solid," *Bulletin of the Seismological Society of America*, Vol. 102, No. 3, 2012, pp. 1224–1234.

[97] Escande, M., Kolluru, P. K., Cléon, L. M., and Sagaut, P., "Lattice Boltzmann Method for wave propagation in elastic solids with a regular lattice: Theoretical analysis and validation," *arXiv preprint arXiv:2009.06404*, 2020.

[98] Zergani, S., Aziz, Z., and Viswanathan, K., "Elastic and Seismic Model for the Generation of Tsunamis via Lattice Boltzmann Method," *Global Journal of Pure and Applied Mathematics*, Vol. 12, No. 3, 2016, pp. 1979–1999.

[99] Mendoza, M. and Munoz, J., "Three-dimensional lattice Boltzmann model for electrodynamics," *Physical Review E*, Vol. 82, No. 5, 2010, pp. 056708.

[100] Hauser, A. and Verhey, J., "Comparison of the lattice-Boltzmann model with the finite-difference time-domain method for electrodynamics," *Physical Review E*, Vol. 99, No. 3, 2019, pp. 033301.

[101] Succi, S., Vergassola, M., and Benzi, R., "Lattice Boltzmann scheme for two-dimensional magnetohydrodynamics," *Physical Review A*, Vol. 43, No. 8, 1991, pp. 4521.

[102] Chen, S., Chen, H., Martnez, D., and Matthaeus, W., "Lattice Boltzmann model for simulation of magnetohydrodynamics," *Physical Review Letters*, Vol. 67, No. 27, 1991, pp. 3776.

[103] Martínez, D. O., Chen, S., and Matthaeus, W. H., "Lattice boltzmann magnetohydrodynamics," *Physics of plasmas*, Vol. 1, No. 6, 1994, pp. 1850–1867.

[104] Dellar, P. J., "Lattice kinetic schemes for magnetohydrodynamics," *Journal of Computational Physics*, Vol. 179, No. 1, 2002, pp. 95–126.

[105] Dellar, P., "Electromagnetic waves in lattice Boltzmann magnetohydrodynamics," *EPL (Europhysics Letters)*, Vol. 90, No. 5, 2010, pp. 50002.

[106] Dellar, P. J., "Lattice Boltzmann formulation for Braginskii magnetohydrodynamics," *Computers & fluids*, Vol. 46, No. 1, 2011, pp. 201–205.

[107] Dellar, P. J., "Lattice Boltzmann magnetohydrodynamics with current-dependent resistivity," *Journal of Computational Physics*, Vol. 237, 2013, pp. 115–131.

[108] De Rosis, A., Liu, R., and Revell, A., "One-stage simplified lattice Boltzmann method for two-and three-dimensional magnetohydrodynamic flows," *Physics of Fluids*, Vol. 33, No. 8, 2021, pp. 085114.

[109] Ma, Y., Dong, S., and Tan, H., "Lattice Boltzmann method for one-dimensional radiation transfer," *Physical Review E*, Vol. 84, No. 1, 2011, pp. 016704.

[110] Liu, X., Huang, Y., Wang, C.-H., and Zhu, K., "Solving steady and transient radiative transfer problems with strong inhomogeneity via a lattice Boltzmann method," *International Journal of Heat and Mass Transfer*, Vol. 155, 2020, pp. 119714.

[111] Liu, X., Wu, H., Zhu, K., and Huang, Y., "Lattice Boltzmann model for multidimensional polarized radiative transfer: theory and application," *Optica*, Vol. 8, No. 9, 2021, pp. 1136–1145.

[112] Mink, A., McHardy, C., Bressel, L., Rauh, C., and Krause, M. J., "Radiative transfer lattice Boltzmann methods: 3D models and their performance in different regimes of radiative transfer," *Journal of Quantitative Spectroscopy and Radiative Transfer*, Vol. 243, 2020, pp. 106810.

[113] Mendoza, M., Boghosian, B., Herrmann, H. J., and Succi, S., "Fast lattice Boltzmann solver for relativistic hydrodynamics," *Physical review letters*, Vol. 105, No. 1, 2010, pp. 014502.

[114] Romatschke, P., Mendoza, M., and Succi, S., "Fully relativistic lattice Boltzmann algorithm," *Physical Review C*, Vol. 84, No. 3, 2011, pp. 034903.

[115] Gabbana, A., Simeoni, D., Succi, S., and Tripiccione, R., "Relativistic lattice Boltzmann methods: Theory and applications," *Physics Reports*, Vol. 863, 2020, pp. 1–63.

[116] Zhou, J., "A lattice Boltzmann model for the shallow water equations," *Computer methods in applied mechanics and engineering*, Vol. 191, No. 32, 2002, pp. 3527–3539.

[117] Zhou, J. G., *Lattice Boltzmann methods for shallow water flows*, Vol. 4, Springer, 2004.

[118] Liu, H., Zhou, J. G., and Burrows, R., "Lattice Boltzmann simulations of the transient shallow water flows," *Advances in Water Resources*, Vol. 33, No. 4, 2010, pp. 387–396.

[119] Peng, Y., Zhou, J., and Burrows, R., "Modelling solute transport in shallow water with the lattice Boltzmann method," *Computers & fluids*, Vol. 50, No. 1, 2011, pp. 181–188.

[120] Venturi, S., Di Francesco, S., Geier, M., and Manciola, P., "A new collision operator for lattice Boltzmann shallow water model: A convergence and stability study," *Advances in Water Resources*, Vol. 135, 2020, pp. 103474.

[121] Sato, K., Kawasaki, K., and Koshimura, S., "A comparative study of the cumulant lattice Boltzmann method in a single-phase free-surface model of violent flows," *Computers & Fluids*, 2022, pp. 105303.

[122] De Rosis, A., "Modeling epidemics by the lattice Boltzmann method," *Physical Review E*, Vol. 102, No. 2, 2020, pp. 023301.

[123] Xue, Y., Liu, P., Tao, Y., and Tang, X., "Abnormal prediction of dense crowd videos by a purpose-driven lattice Boltzmann model," *International Journal of Applied Mathematics and Computer Science*, Vol. 27, No. 1, 2017, pp. 181–194.

[124] Tao, Y., Liu, P., Zhao, W., and Tang, X., "Forecasting Crowd State in Video by an Improved Lattice Boltzmann Model," *International Conference on Neural Information Processing*, Springer, 2014, pp. 50–57.

[125] Coreixas, C., Wissocq, G., Puigt, G., Boussuge, J.-F., and Sagaut, P., "Recursive regularization step for high-order lattice Boltzmann methods," *Physical Review E*, Vol. 96, No. 3, 2017, pp. 033306.

[126] Coreixas, C., Wissocq, G., Chopard, B., and Latt, J., "Impact of collision models on the physical properties and the stability of lattice Boltzmann methods," *Philosophical Transactions of the Royal Society A*, Vol. 378, No. 2175, 2020, pp. 20190397.

[127] Wissocq, G. and Sagaut, P., "Hydrodynamic limits and numerical errors of isothermal lattice Boltzmann schemes," *Journal of Computational Physics*, Vol. 450, 2022, pp. 110858.

[128] Masset, P.-A. and Wissocq, G., "Linear hydrodynamics and stability of the discrete velocity Boltzmann equations," *Journal of Fluid Mechanics*, Vol. 897, 2020.

[129] Farag, G., Zhao, S., Chiavassa, G., and Boivin, P., "Consistency study of lattice-Boltzmann schemes macroscopic limit," *Physics of Fluids*, Vol. 33, No. 3, 2021, pp. 037101.

[130] Farag, G., *Lattice Boltzmann Methods for compressible flows*, Ph.D. thesis, Aix-Marseille Université, 2022.

[131] Philippi, P. C., Hegele Jr, L. A., Dos Santos, L. O., and Surmas, R., "From the continuous to the lattice Boltzmann equation: The discretization problem and thermal models," *Physical Review E*, Vol. 73, No. 5, 2006, pp. 056702.

[132] Dimarco, G. and Loubere, R., "Towards an ultra efficient kinetic scheme. Part I: Basics on the BGK equation," *Journal of Computational Physics*, Vol. 255, 2013, pp. 680–698.

[133] Dimarco, G. and Loubere, R., "Towards an ultra efficient kinetic scheme. Part II: The high order case," *Journal of Computational Physics*, Vol. 255, 2013, pp. 699–719.

[134] Dimarco, G., Loubère, R., and Narski, J., "Towards an ultra efficient kinetic scheme. Part III: High-performance-computing," *Journal of Computational Physics*, Vol. 284, 2015, pp. 22–39.

[135] Xu, K., "A gas-kinetic BGK scheme for the Navier–Stokes equations and its connection with artificial dissipation and Godunov method," *Journal of Computational Physics*, Vol. 171, No. 1, 2001, pp. 289–335.

[136] Xu, K. and Huang, J.-C., "A unified gas-kinetic scheme for continuum and rarefied flows," *Journal of Computational Physics*, Vol. 229, No. 20, 2010, pp. 7747–7764.

[137] Guo, Z. and Xu, K., "Progress of discrete unified gas-kinetic scheme for multiscale flows," *Advances in Aerodynamics*, Vol. 3, No. 1, 2021, pp. 1–42.

[138] Xu, K., *Direct modeling for computational fluid dynamics: construction and application of unified gas-kinetic schemes*, Vol. 4, World Scientific, 2014.

[139] Chen, H. and Shan, X., "Fundamental conditions for N-th-order accurate lattice Boltzmann models," *Physica D: Nonlinear Phenomena*, Vol. 237, No. 14-17, 2008, pp. 2003–2008.

[140] Chikatamarla, S. S. and Karlin, I. V., "Lattices for the lattice Boltzmann method," *Physical Review E*, Vol. 79, No. 4, 2009, pp. 046701.

[141] Shan, X., "The mathematical structure of the lattices of the lattice Boltzmann method," *Journal of Computational Science*, Vol. 17, 2016, pp. 475–481.

[142] Shan, X. et al., "General solution of lattices for Cartesian lattice Bhatanagar-Gross-Krook models," *Physical Review E*, Vol. 81, No. 3, 2010, pp. 036702.

[143] Rubinstein, R. and Luo, L.-S., "Theory of the lattice Boltzmann equation: Symmetry properties of discrete velocity sets," *Physical Review E*, Vol. 77, No. 3, 2008, pp. 036709.

[144] Ubertini, S., Asinari, P., and Succi, S., "Three ways to lattice Boltzmann: a unified time-marching picture," *Physical Review E*, Vol. 81, No. 1, 2010, pp. 016311.

[145] Guo, Z., Zhao, T., and Shi, Y., "A lattice Boltzmann algorithm for electro-osmotic flows in microfluidic devices," *The Journal of chemical physics*, Vol. 122, No. 14, 2005, pp. 144907.

[146] Chai, Z. and Shi, B., "A novel lattice Boltzmann model for the Poisson equation," *Applied mathematical modelling*, Vol. 32, No. 10, 2008, pp. 2050–2058.

[147] Chopard, B., Falcone, J. L., and Latt, J., "The lattice Boltzmann advection-diffusion model revisited," *The European Physical Journal Special Topics*, Vol. 171, No. 1, 2009, pp. 245–249.

[148] Velasco, A. M., Muñoz, J. D., and Mendoza, M., "Lattice Boltzmann model for the simulation of the wave equation in curvilinear coordinates," *Journal of Computational Physics*, Vol. 376, 2019, pp. 76–97.

[149] Yan, G., "A Lattice Boltzmann equation for the simulation waves," *Journal of Computational Physics*, Vol. 161, 2000, pp. 61–69.

[150] Yan, B. and Yan, G., "A steady-state Lattice Boltzmann model for incompressible flows," *Computers and Mathematics with Applications*, Vol. 61, 2011, pp. 1348–1354.

[151] Chen, S., Tölke, J., and Krafczyk, M., "A new method for the numerical solution of vorticity–streamfunction formulations," *Computer Methods in Applied Mechanics and Engineering*, Vol. 198, No. 3-4, 2008, pp. 367–376.

[152] Ljubomir, B., "Quantum algorithm for the Navier–Stokes equations by using the streamfunction-vorticity formulation and the lattice Boltzmann method," *International Journal of Quantum Information*, 2022, pp. 2150039.

[153] Chen, H., Zhang, R., and Gopalakrishnan, P., "Filtered lattice Boltzmann collision formulation enforcing isotropy and Galilean invariance," *Physica Scripta*, Vol. 95, No. 3, 2020, pp. 034003.

[154] Mattila, K. K., Philippi, P. C., and Hegele Jr, L. A., "High-order regularization in lattice-Boltzmann equations," *Physics of Fluids*, Vol. 29, No. 4, 2017, pp. 046103.

[155] Latt, J. and Chopard, B., "Lattice Boltzmann method with regularized pre-collision distribution functions," *Mathematics and Computers in Simulation*, Vol. 72, No. 2-6, 2006, pp. 165–168.

[156] Zhang, R., Shan, X., and Chen, H., "Efficient kinetic method for fluid simulation beyond the Navier-Stokes equation," *Physical Review E*, Vol. 74, No. 4, 2006, pp. 046703.

[157] Brogi, F., Malaspinas, O., Chopard, B., and Bonadonna, C., "Hermite regularization of the lattice Boltzmann method for open source computational aeroacoustics," *The Journal of the Acoustical Society of America*, Vol. 142, No. 4, 2017, pp. 2332–2345.

[158] Jacob, J., Malaspinas, O., and Sagaut, P., "A new hybrid recursive regularised Bhatnagar–Gross–Krook collision model for lattice Boltzmann method-based large eddy simulation," *Journal of Turbulence*, Vol. 19, No. 11-12, 2018, pp. 1051–1076.

[159] Krämer, A., Wilde, D., Küllmer, K., Reith, D., and Foysi, H., "Pseudoentropic derivation of the regularized lattice Boltzmann method," *Physical Review E*, Vol. 100, No. 2, 2019, pp. 023302.

[160] Guo, S., Feng, Y., and Sagaut, P., "Improved standard thermal lattice Boltzmann model with hybrid recursive regularization for compressible laminar and turbulent flows," *Physics of Fluids*, Vol. 32, No. 12, 2020, pp. 126108.

[161] Geier, M., Greiner, A., and Korvink, J. G., "Cascaded digital lattice Boltzmann automata for high Reynolds number flow," *Physical Review E*, Vol. 73, No. 6, 2006, pp. 066705.

[162] Geier, M., Greiner, A., and Korvink, J. G., "A factorized central moment lattice Boltzmann method," *The European Physical Journal Special Topics*, Vol. 171, No. 1, 2009, pp. 55–61.

[163] De Rosis, A. and Luo, K. H., "Role of higher-order Hermite polynomials in the central-moments-based lattice Boltzmann framework," *Physical Review E*, Vol. 99, No. 1, 2019, pp. 013301.

[164] Dubois, F., Fevrier, T., and Graille, B., "Lattice Boltzmann schemes with relative velocities," *Communications in Computational Physics*, Vol. 17, No. 4, 2015, pp. 1088–1112.

[165] Geier, M., Schönherr, M., Pasquali, A., and Krafczyk, M., "The cumulant lattice Boltzmann equation in three dimensions: Theory and validation," *Computers & Mathematics with Applications*, Vol. 70, No. 4, 2015, pp. 507–547.

[166] Seeger, S. and Hoffmann, H., "The cumulant method for computational kinetic theory," *Continuum Mechanics and Thermodynamics*, Vol. 12, No. 6, 2000, pp. 403–421.

[167] Geier, M., Pasquali, A., and Schönherr, M., "Parametrization of the cumulant lattice Boltzmann method for fourth order accurate diffusion part I: Derivation and validation," *Journal of Computational Physics*, Vol. 348, 2017, pp. 862–888.

[168] Geier, M. and Pasquali, A., "Fourth order Galilean invariance for the lattice Boltzmann method," *Computers & Fluids*, Vol. 166, 2018, pp. 139–151.

[169] Coreixas, C., Chopard, B., and Latt, J., "Comprehensive comparison of collision models in the lattice Boltzmann framework: Theoretical investigations," *Physical Review E*, Vol. 100, No. 3, 2019, pp. 033305.

[170] Asinari, P., "Generalized local equilibrium in the cascaded lattice Boltzmann method," *Physical Review E*, Vol. 78, No. 1, 2008, pp. 016701.

[171] Brownlee, R., Gorban, A. N., and Levesley, J., "Stability and stabilization of the lattice Boltzmann method," *Physical Review E*, Vol. 75, No. 3, 2007, pp. 036711.

[172] Brownlee, R. A., Levesley, J., Packwood, D., and Gorban, A. N., "Add-ons for lattice Boltzmann methods: Regularization, filtering and limiters," *Novel Trends in Lattice-Boltzmann Methods*, 2013, pp. 31.

[173] Karlin, I. V., Gorban, A. N., Succi, S., and Boffi, V., "Maximum entropy principle for lattice kinetic equations," *Physical Review Letters*, Vol. 81, No. 1, 1998, pp. 6.

[174] Karlin, I. V., Ferrante, A., and Öttinger, H. C., "Perfect entropy functions of the lattice Boltzmann method," *EPL (Europhysics Letters)*, Vol. 47, No. 2, 1999, pp. 182.

[175] Ansumali, S. and Karlin, I. V., "Stabilization of the lattice Boltzmann method by the H theorem: A numerical test," *Physical Review E*, Vol. 62, No. 6, 2000, pp. 7999.

[176] Succi, S., Karlin, I. V., and Chen, H., "Colloquium: Role of the H theorem in lattice Boltzmann hydrodynamic simulations," *Reviews of Modern Physics*, Vol. 74, No. 4, 2002, pp. 1203.

[177] Ansumali, S. and Karlin, I. V., "Single relaxation time model for entropic lattice Boltzmann methods," *Physical Review E*, Vol. 65, No. 5, 2002, pp. 056312.

[178] Ansumali, S., Karlin, I. V., and Öttinger, H. C., "Minimal entropic kinetic models for hydrodynamics," *EPL (Europhysics Letters)*, Vol. 63, No. 6, 2003, pp. 798.

[179] Boghosian, B. M., Love, P. J., Coveney, P. V., Karlin, I. V., Succi, S., and Yepez, J., "Galilean-invariant lattice-Boltzmann models with H theorem," *Physical Review E*, Vol. 68, No. 2, 2003, pp. 025103.

[180] Ansumali, S. and Karlin, I. V., "Consistent lattice Boltzmann method," *Physical review letters*, Vol. 95, No. 26, 2005, pp. 260605.

[181] Chikatamarla, S., Ansumali, S., and Karlin, I. V., "Entropic lattice Boltzmann models for hydrodynamics in three dimensions," *Physical review letters*, Vol. 97, No. 1, 2006, pp. 010201.

[182] Prasianakis, N., Chikatamarla, S. S., Karlin, I. V., Ansumali, S., and Boulouchos, K., "Entropic lattice Boltzmann method for simulation of thermal flows," *Mathematics and Computers in Simulation*, Vol. 72, No. 2-6, 2006, pp. 179–183.

[183] Brownlee, R., Gorban, A. N., and Levesley, J., "Stabilization of the lattice Boltzmann method using the Ehrenfests coarse-graining idea," *Physical Review E*, Vol. 74, No. 3, 2006, pp. 037703.

[184] Keating, B., Vahala, G., Yepez, J., Soe, M., and Vahala, L., "Entropic lattice Boltzmann representations required to recover Navier-Stokes flows," *Physical Review E*, Vol. 75, No. 3, 2007, pp. 036712.

[185] Brownlee, R., Gorban, A. N., and Levesley, J., "Nonequilibrium entropy limiters in lattice Boltzmann methods," *Physica A: Statistical Mechanics and its Applications*, Vol. 387, No. 2-3, 2008, pp. 385–406.

[186] Asinari, P. and Karlin, I. V., "Generalized Maxwell state and H theorem for computing fluid flows using the lattice Boltzmann method," *Physical Review E*, Vol. 79, No. 3, 2009, pp. 036703.

[187] Atif, M., Kolluru, P. K., Thantanapally, C., and Ansumali, S., "Essentially entropic lattice Boltzmann model," *Physical review letters*, Vol. 119, No. 24, 2017, pp. 240602.

[188] Xie, C., Lei, W., and Wang, M., "Lattice Boltzmann model for three-phase viscoelastic fluid flow," *Physical Review E*, Vol. 97, No. 2, 2018, pp. 023312.

[189] Su, J., Ouyang, J., Wang, X., and Yang, B., "Lattice Boltzmann method coupled with the Oldroyd-B constitutive model for a viscoelastic fluid," *Physical Review E*, Vol. 88, No. 5, 2013, pp. 053304.

[190] Zou, S., Yuan, X.-F., Yang, X., Yi, W., and Xu, X., "An integrated lattice Boltzmann and finite volume method for the simulation of viscoelastic fluid flows," *Journal of Non-Newtonian Fluid Mechanics*, Vol. 211, 2014, pp. 99–113.

[191] Su, J., Ouyang, J., and Lu, J., "A Lattice Boltzmann Method and Asynchronous Model Coupling for Viscoelastic Fluids," *Applied Sciences*, Vol. 8, No. 3, 2018, pp. 352.

[192] Feng, Y., Boivin, P., Jacob, J., and Sagaut, P., "Hybrid recursive regularized lattice Boltzmann simulation of humid air with application to meteorological flows," *Physical Review E*, Vol. 100, No. 2, 2019, pp. 023304.

[193] Dubois, F. and Lallemand, P., "Towards higher order lattice Boltzmann schemes," *Journal of Statistical mechanics: theory and experiment*, Vol. 2009, No. 06, 2009, pp. P06006.

[194] Dubois, F. and Lallemand, P., "Quartic parameters for acoustic applications of lattice Boltzmann scheme," *Computers & Mathematics with Applications*, Vol. 61, No. 12, 2011, pp. 3404–3416.

[195] Dubois, F., Lallemand, P., and Tekitek, M. M., "Taylor expansion method for linear lattice Boltzmann schemes with an external force: application to boundary conditions," *High Order Nonlinear Numerical Schemes for Evolutionary PDEs*, Springer, 2014, pp. 89–107.

[196] Sterling, J. D. and Chen, S., "Stability analysis of lattice Boltzmann methods," *Journal of Computational Physics*, Vol. 123, No. 1, 1996, pp. 196–206.

[197] Marié, S., Ricot, D., and Sagaut, P., "Comparison between lattice Boltzmann method and Navier–Stokes high order schemes for computational aeroacoustics," *Journal of Computational Physics*, Vol. 228, No. 4, 2009, pp. 1056–1070.

[198] Xu, H., Malaspinas, O., and Sagaut, P., "Sensitivity analysis and determination of free relaxation parameters for the weakly-compressible MRT–LBM schemes," *Journal of Computational Physics*, Vol. 231, No. 21, 2012, pp. 7335–7367.

[199] Hosseini, S. A., Coreixas, C., Darabiha, N., and Thévenin, D., "Stability of the lattice kinetic scheme and choice of the free relaxation parameter," *Physical Review E*, Vol. 99, No. 6, 2019, pp. 063305.

[200] Wissocq, G., Coreixas, C., and Boussuge, J.-F., "Linear stability and isotropy properties of athermal regularized lattice Boltzmann methods," *Physical Review E*, Vol. 102, No. 5, 2020, pp. 053305.

[201] Renard, F., Wissocq, G., Boussuge, J.-F., and Sagaut, P., "A linear stability analysis of compressible hybrid lattice Boltzmann methods," *Journal of Computational Physics*, Vol. 446, 2021, pp. 110649.

[202] Wissocq, G., Sagaut, P., and Boussuge, J.-F., "An extended spectral analysis of the lattice Boltzmann method: modal interactions and stability issues," *Journal of Computational Physics*, Vol. 380, 2019, pp. 311–333.

[203] Sagaut, P. and Cambon, C., *Homogeneous turbulence dynamics, second edition*, Springer, 2018.

[204] Barenghi, C. F., Donnelly, R. J., and Vinen, W., *Quantized vortex dynamics and superfluid turbulence*, Vol. 571, Springer Science & Business Media, 2001.

[205] Vinen, W. and Niemela, J., "Quantum turbulence," *Journal of low temperature physics*, Vol. 128, No. 5, 2002, pp. 167–231.

[206] Paoletti, M. S. and Lathrop, D. P., "Quantum turbulence," *Annu. Rev. Condens. Matter Phys.*, Vol. 2, No. 1, 2011, pp. 213–234.

[207] Nemirovskii, S. K., "Quantum turbulence: Theoretical and numerical problems," *Physics Reports*, Vol. 524, No. 3, 2013, pp. 85–202.

[208] Tsubota, M., Fujimoto, K., and Yui, S., "Numerical studies of quantum turbulence," *Journal of Low Temperature Physics*, Vol. 188, No. 5, 2017, pp. 119–189.

[209] Succi, S. and Benzi, R., "Lattice Boltzmann equation for quantum mechanics," *Physica D: Nonlinear Phenomena*, Vol. 69, No. 3-4, 1993, pp. 327–332.

[210] Succi, S., "Numerical solution of the Schrödinger equation using discrete kinetic theory," *Physical Review E*, Vol. 53, No. 2, 1996, pp. 1969.

[211] Palpacelli, S. and Succi, S., "The quantum Lattice Boltzmann equation: recent developments," *Communications in Computational Physics*, Vol. 4, No. 5, 2008, pp. 980–1007.

[212] Lapitski, D. and Dellar, P. J., "Convergence of a three-dimensional quantum lattice Boltzmann scheme towards solutions of the Dirac equation," *Philosophical Transactions of the Royal Society A: Mathematical, Physical and Engineering Sciences*, Vol. 369, No. 1944, 2011, pp. 2155–2163.

[213] Dellar, P. J., "An exact energy conservation property of the quantum lattice Boltzmann algorithm," *Physics Letters A*, Vol. 376, No. 1, 2011, pp. 6–13.

[214] Colmenares, M. A. V. and Castano, J. D. M., "Numerical comparison of 1D quantum lattice Boltzmann models," *Journal of Statistical Mechanics: Theory and Experiment*, Vol. 2009, No. 06, 2009, pp. P06004.

[215] Palpacelli, S., *Quantum lattice Boltzmann methods for the linear and nonlinear Schrödinger equation in several dimensions*, Ph.D. thesis, Università degli studi Roma Tre, 2009.

[216] Yepez, J., "Lattice-gas quantum computation," *International Journal of Modern Physics C*, Vol. 9, No. 08, 1998, pp. 1587–1596.

[217] Yepez, J., "Quantum lattice-gas model for computational fluid dynamics," *Physical Review E*, Vol. 63, No. 4, 2001, pp. 046702.

[218] Yepez, J., "Quantum lattice-gas model for the diffusion equation," *International Journal of Modern Physics C*, Vol. 12, No. 09, 2001, pp. 1285–1303.

[219] Yepez, J., "Quantum lattice-gas model for the Burgers equation," *Journal of Statistical Physics*, Vol. 107, No. 1, 2002, pp. 203–224.

[220] Yepez, J. and Boghosian, B., "An efficient and accurate quantum lattice-gas model for the many-body Schrödinger wave equation," *Computer Physics Communications*, Vol. 146, No. 3, 2002, pp. 280–294.

[221] Yepez, J., Vahala, G., and Vahala, L., "Lattice quantum algorithm for the Schrödinger wave equation in 2+ 1 dimensions with a demonstration by modeling soliton instabilities," *Quantum Information Processing*, Vol. 4, No. 6, 2005, pp. 457–469.

[222] Yepez, J., Vahala, G., Vahala, L., and Soe, M., "Superfluid turbulence from quantum Kelvin wave to classical Kolmogorov cascades," *Physical Review Letters*, Vol. 103, No. 8, 2009, pp. 084501.

[223] Vahala, G., Yepez, J., and Vahala, L., "Quantum lattice gas representation of some classical solitons," *Physics Letters A*, Vol. 310, No. 2-3, 2003, pp. 187–196.

[224] Vahala, L., Vahala, G., and Yepez, J., "Lattice Boltzmann and quantum lattice gas representations of one-dimensional magnetohydrodynamic turbulence," *Physics Letters A*, Vol. 306, No. 4, 2003, pp. 227–234.

[225] Vahala, G., Yepez, J., Vahala, L., Soe, M., Zhang, B., and Ziegeler, S., "Poincaré recurrence and spectral cascades in three-dimensional quantum turbulence," *Physical Review E*, Vol. 84, No. 4, 2011, pp. 046713.

[226] Vahala, G., Yepez, J., Vahala, L., and Soe, M., "Unitary qubit lattice simulations of complex vortex structures," *Computational Science & Discovery*, Vol. 5, No. 1, 2012, pp. 014013.

[227] Vahala, G., Zhang, B., Yepez, J., Vahala, L., and Soe, M., *Unitary qubit lattice gas representation of 2D and 3D quantum turbulence*, InTech Publishers: Croatia, 2012.

[228] Oganesov, A., Vahala, G., Vahala, L., Yepez, J., and Soe, M., "Benchmarking the Dirac-generated unitary lattice qubit collision-stream algorithm for 1D vector Manakov soliton collisions," *Computers & Mathematics with Applications*, Vol. 72, No. 2, 2016, pp. 386–393.

[229] Vahala, L., Vahala, G., Soe, M., Ram, A., and Yepez, J., "Unitary qubit lattice algorithm for three-dimensional vortex solitons in hyperbolic self-defocusing media," *Communications in Nonlinear Science and Numerical Simulation*, Vol. 75, 2019, pp. 152–159.

[230] Wang, H., "Numerical simulation for the Gross-Pitaevskii equation based on the lattice Boltzmann method," *Advances in Space Research*, Vol. 60, No. 6, 2017, pp. 1261–1270.

[231] Inui, S. and Tsubota, M., "Coupled dynamics of quantized vortices and normal fluid in superfluid He 4 based on the lattice Boltzmann method," *Physical Review B*, Vol. 104, No. 21, 2021, pp. 214503.

[232] Bertolaccini, J., Lévêque, E., and Roche, P.-E., "Disproportionate entrance length in superfluid flows and the puzzle of counterflow instabilities," *Physical Review Fluids*, Vol. 2, No. 12, 2017, pp. 123902.

[233] Todorova, B. and Steijl, R., "Quantum algorithm for the collisionless Boltzmann equation," *Journal of Computational Physics*, Vol. 409, 2020, pp. 109347.

[234] Budinski, L., "Quantum algorithm for the advection-diffusion equation simulated with the lattice Boltzmann method," *Quantum Information Processing*, Vol. 20, 2021, pp. 1–17.

[235] Chen, Z., Yepez, J., and Cory, D. G., "Simulation of the Burgers equation by NMR quantum-information processing," *Phys. Rev. A*, Vol. 74, Oct 2006, pp. 042321.

[236] Love, P., "On quantum extensions of hydrodynamic lattice gas automata," *Condensed Matter*, Vol. 4, pp. 48.